The Segmented Zambezi Sedimentary System from Source to Sink: 1. Sand Petrology and Heavy Minerals

Eduardo Garzanti,[1,*] *Guido Pastore,*[1] *Alberto Resentini,*[1] *Giovanni Vezzoli,*[1] *Pieter Vermeesch,*[2] *Lindani Ncube,*[3] *Helena Johanna Van Niekerk,*[3] *Gwenael Jouet,*[4] *and Massimo Dall'Asta*[5]

1. Laboratory for Provenance Studies, Department of Earth and Environmental Sciences, University of Milano-Bicocca, 20126 Milan, Italy; 2. London Geochronology Centre, Department of Earth Sciences, University College London, London WC1E 6BT, United Kingdom; 3. Department of Environmental Sciences, University of South Africa, Florida, South Africa; 4. Unité de Recherche Geosciences Marines, IFREMER (Institut Français de Recherche pour l'Exploitation de la Mer), CS 10070, 29280 Plouzané, France; 5. TOTAL Exploration and Production, CSTJF, Avenue Larribau, 64018 Pau Cedex, France

ABSTRACT

The Zambezi River rises at the center of southern Africa, flows across the low-relief Kalahari Plateau, meets Karoo basalt, plunges into Victoria Falls, follows along Karoo rifts, and pierces through Precambrian basement to eventually deliver its load onto the Mozambican passive margin. Reflecting its polyphase evolution, the river is subdivided into segments with different geological and geomorphological character, a subdivision finally fixed by man's construction of large reservoirs and faithfully testified by sharp changes in sediment composition. Pure quartzose sand recycled from Kalahari desert dunes in the uppermost tract is next progressively enriched in basaltic rock fragments and clinopyroxene. Sediment load is renewed first downstream of Lake Kariba and next downstream of Lake Cahora Bassa, documenting a stepwise decrease in quartz and durable heavy minerals. Composition becomes quartzo-feldspathic in the lower tract, where most sediment is supplied by high-grade basements rejuvenated by the southward propagation of the East African rift. Feldspar abundance in Lower Zambezi sand has no equivalent among big rivers on Earth and far exceeds that in sediments of the northern delta, shelf, and slope, revealing that provenance signals from the upper reaches have ceased to be transmitted across the routing system after closure of the big dams. This high-resolution petrologic study of Zambezi sand allows us to critically reconsider several dogmas, such as the supposed increase of mineralogical "maturity" during long-distance fluvial transport, and forges a key to unlock the rich information stored in sedimentary archives, with the ultimate goal to accurately reconstruct the evolution of this mighty river flowing across changing African landscapes since the late Mesozoic.

Online enhancements: appendix tables.

A river or a drainage basin might best be considered to have a heritage rather than an origin. It is like an organic form, the product of a continuous evolutionary line through time. (Leopold et al. 1995, p. 421)

Nyaminyami is a personification of the Zambezi itself and, by analogy, of the life force and the will to survive. (Main 1990, p. 124)

Manuscript received December 15, 2020; accepted May 10, 2021; electronically published September 7, 2021.

* Author for correspondence; email: eduardo.garzanti@unimib.it.

Introduction

The Zambezi is one of the most fascinating river systems on Earth, flowing across wild landscapes from Barotseland to Victoria Falls and next plunging into deep gorges carved in basalt and along ancient rift valleys to finally reach the Indian Ocean (fig. 1; Main 1990; Moore et al. 2007). The relatively recent, complex, and controversial natural evolution of its drainage basin ended in the Anthropocene with its drastic subdivision into separate segments by man's construction of two big dams and associated reservoirs.

This is the first of a series of articles aiming at characterizing, by a multitechnique approach,

Journal of Geology, volume 129, number 4, July 2021. https://doi.org/10.1086/715792

Figure 1. Zambezi drainage basin (base map from Google Earth). White circles indicate sampling locations (more information in file Zambezi.kmz). VF = Victoria Falls.

the composition of sediment generated in the diverse tracts of the vast Zambezi catchment and the present and inherited factors that influence compositional variability from the headwaters to the Mozambican coast and beyond. This study, based on framework petrography and heavy-mineral data, focuses specifically on: (1) the relative effects of source-rock lithology and chemical weathering on sand mineralogy in a subequatorial climate, (2) the transmission of compositional signals along the sediment-routing system from source to sink, and (3) the use and misuse of current petrological models to infer sediment provenance and of mineralogical parameters to infer climatic conditions. A forthcoming companion article will be based on complementary data from sand and mud geochemistry, clay mineralogy, and detrital zircon geochronology on the same sample set (Garzanti et al. forthcoming). Our ultimate purpose is to build up a solid knowledge of the modern sedimentary system that can be applied to trace fluvial transport from the land to the deep sea and, eventually, to investigate provenance changes recorded in stratigraphic successions accumulated in marine depocenters through time and thus unravel the complex evolution of the Zambezi River since the late Mesozoic.

Geology

The Precambrian. The Archean core of southern Africa includes the Zimbabwe Craton, welded by the Limpopo Belt to the Kaapvaal Craton in the south and bounded by the mid-Paleoproterozoic Magondi Belt in the west (fig. 2). The Zimbabwe Craton comprises a central terrane flanked by greenstone belts. Gneisses of the central terrane are nonconformably overlain by volcanic rocks and conglomerates. The craton was stabilized in the mid-Neoarchean and finally sealed by the Great Dike Swarm at ~2575 Ma (Jelsma and Dirks 2002; Söderlund et al. 2010).

The composite Archean core grew progressively during the Paleoproterozoic and Mesoproterozoic. The Proto-Kalahari Craton was established by the late Paleoproterozoic and affected by widespread intraplate magmatism at 1.1 Ga (Hanson et al. 2006), not long before the Kalahari Craton was formed during the orogenic event when Rodinia was assembled (Jacobs et al. 2008).

Orogens developed in the Paleoproterozoic and reworked in the Neoproterozoic at the southern margin of the Tanzania Craton include the northwest-southeast-trending Ubendian metamorphic belt,

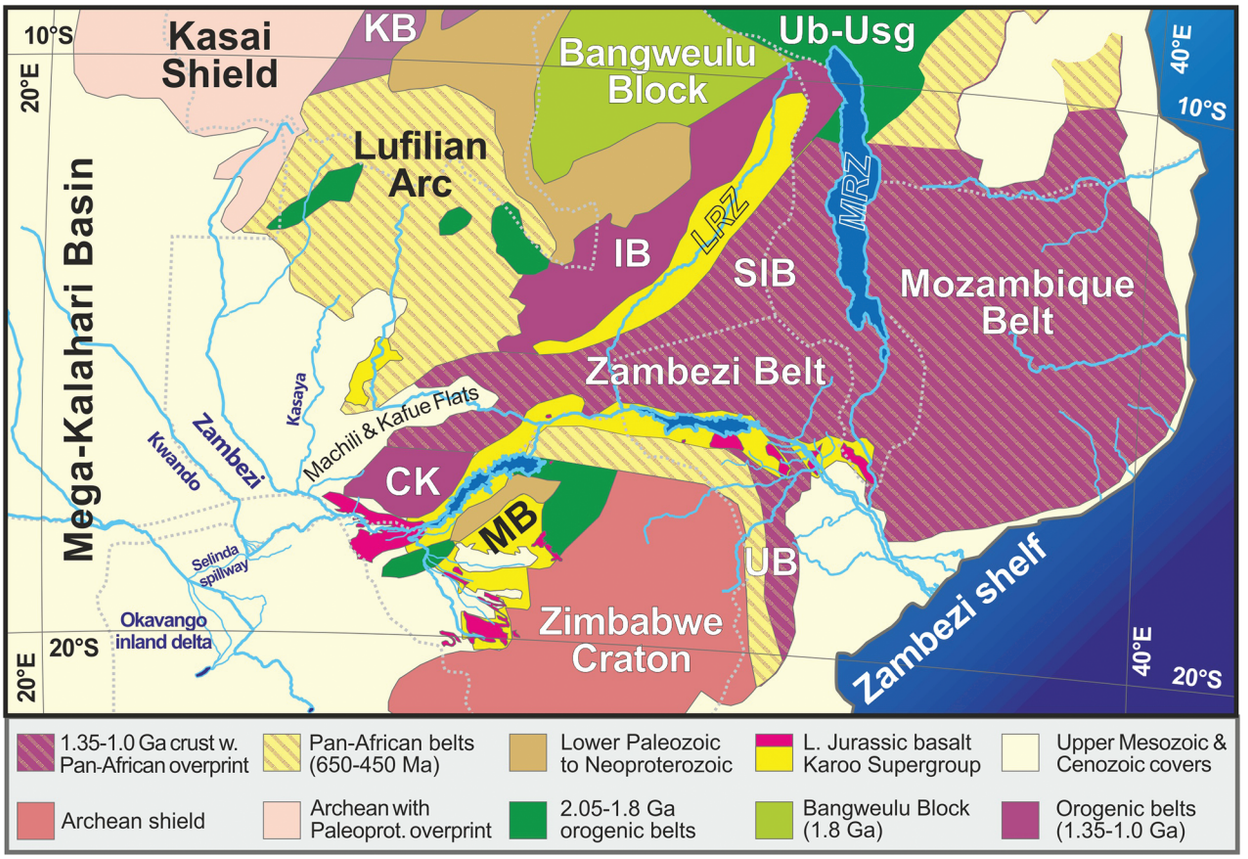

Figure 2. Geological domains in Zambezi catchment and adjacent regions (after Hanson 2003 and Thiéblemont et al. 2016). CK = Choma-Kalomo Block; IB = Irumide Belt; KB = Kibaran Belt; LRZ = Luangwa Rift Zone, activated in the Permian and reactivated in the Neogene; MB = Magondi Belt; MRZ = Malawi Rift Zone; SIB = South Irumide Belt, deeply affected by the Pan-African orogeny; UB = Umkondo Belt; Ub-Usg = Ubendian-Usagaran Belts; L. Jurassic = Lower Jurassic; Paleoprot. = Paleoproterozoic.

bounding the Bangweulu Block to the north (Boniface and Appel 2018) and the southwest-northeast-striking Usagaran Belt to the east (Collins et al. 2004). In northern Zimbabwe, the Orosirian Magondi Belt contains arc-related volcano-sedimentary and plutonic rocks metamorphosed at amphibolite facies (Majaule et al. 2001; Master et al. 2010).

Orogens generated in the Mesoproterozoic include the Kibaran Belt in the north (Kokonyangi et al. 2006; Debruyne et al. 2015) and the Irumide Belt, which stretches from central Zambia in the southwest to northern Malawi in the northeast, is delimited by the largely undeformed basement of the Bangweulu Block in the north, and was largely affected by the Neoproterozoic orogeny in the west (fig. 2). The Irumide Belt includes a Paleoproterozoic gneissic basement overlain by siliciclastic and minor carbonate strata deposited during the late Orosirian (Muva Supergroup), as well as granitoid suites emplaced in the earliest, middle, and latest Mesoproterozoic. During the ~1 Ga orogeny, metamorphic grade increased from greenschist facies in the northwest to upper amphibolite and granulite facies in the southeast (De Waele et al. 2006, 2009). The Choma-Kalomo Block in southern Zambia is a distinct Mesoproterozoic domain also including amphibolite-facies metasediments and granitoid intrusions affected by the latest Mesoproterozoic thermal event (Glynn et al. 2017).

The Kalahari Craton of southern Africa was finally welded to the Congo Craton during the major Neoproterozoic Pan-African orogeny, testified by the Damara-Lufilian-Zambezi Belt stretching from coastal Namibia in the west and across Botswana and southern Zambia to finally connect with the Mozambique Belt in the east (Frimmel et al. 2011; Fritz et al. 2013; Goscombe et al. 2020). The Lufilian Arc, located between the Congo and Kalahari

Cratons, consists of Neoproterozoic low-to-high-grade metasedimentary and metaigneous rocks hosting Cu-Co-U and Pb-Zn mineralizations (Kampunzu and Cailteux 1999; John et al. 2004; Eglinger et al. 2016). The Zambezi Belt contains a volcano-sedimentary succession deformed under amphibolite-facies conditions during the early Neoproterozoic (Hanson 2003), whereas eclogite-facies metamorphism constrains the timing of subduction and basin closure as latest Neoproterozoic (Hargrove et al. 2003; John et al. 2003).

The Breakup of Gondwana. A major tectono-magmatic event straddling the Paleozoic/Mesozoic boundary is widely documented across southern Africa (Jourdan et al. 2005; Manninen et al. 2008), when the several kilometer-thick Upper Carboniferous to Lower Jurassic Karoo Supergroup was deposited, including glacial sediments, shale, and volcaniclastic sandstone followed by fluvial sediments (Johnson et al. 1996). Sedimentation was influenced by changing climate, from initially cold to warmer since the mid-Permian and finally hot with fluctuating precipitation in the Triassic, when braidplain sandstone and floodplain mudstone were capped by eolian sandstone (Catuneanu et al. 2005). Karoo-type basins formed in intra- and intercratonic settings by rift-related extension. In the Tuli and mid-Zambezi basins of Zimbabwe, glacial deposits are overlain by Permian sandstones and coal-bearing mudrocks, followed by ~0.5-km-thick Triassic red beds and pebbly sandstones (Bicca et al. 2017). Karoo sedimentation was terminated by flood-basalt eruptions recorded throughout southern Africa in the Early Jurassic (Svensen et al. 2012).

Finally, rifting and breakup of Gondwana in the mid-Jurassic was followed by opening of the Indian Ocean in the Early Cretaceous, an event associated with formation of sedimentary basins (Salman and Abdula 1995; Walford et al. 2005), strike-slip deformation (Klimke et al. 2016), and extensive volcanism in the Mozambique Channel (Vallier 1974; König and Jokat 2010).

In the Cenozoic, fluvial and lacustrine sediments were deposited inland in the Mega-Kalahari rim basin (in Tswana language *Kgalagadi*, "waterless place"), which comprises the largest sand sea on Earth, extending across the southern Africa plateau for more than 2.5×10^6 km^2 (Haddon and McCarthy 2005). Repeated phases of eolian deposition took place during Quaternary dry stages, separated by depositional hiatuses corresponding to more humid stages (Stokes et al. 1998; Thomas and Shaw 2002). The East African rift developed throughout the Neogene (Ebinger and Scholz 2012; Roberts et al. 2012; Maselli et al. 2019), until along-axis propagation reached the Kalahari region in the Quaternary, through a network of unconnected basins extending southwest of Lake Tanganyika (Kinabo et al. 2007). Since the late Pleistocene, faulting and subsidence in the incipient Okavango Rift Zone has exerted a major control on drainage reorganization.

The Zambezi River

The Zambezi (from either the Bantu term *mbeze*, "fish," or the M'biza people of central–eastern Zambia), 2575 km in length and with a catchment area of ~1.4×10^6 km^2, is the largest river of southern Africa, extending from 11° to 20°S and from 19°E to 36°30′E (fig. 1). Annual water discharge is ~100 km^3, and suspended load amounts to 50–100 million tons (Hay 1998). Annual rainfall in the basin increases from <600 mm in the south to >1200 mm in the north. The largest contribution to runoff, therefore, comes from the headwater branches in Zambia and Angola. Mean monthly flows at Victoria Falls remain more than 1000 m^3/s from February to June, with maxima of 3000 m^3/s in April and minima of 300 m^3/s in October to November; 9000 m^3/s were reached during the 1958 flood, while the Kariba Dam was under construction (Moore et al. 2007).

The natural course of the Zambezi River has been modified profoundly by the great dams that have created since 1959 Lake Kariba, marking the border between Zimbabwe and Zambia, and since 1974 Lake Cahora Bassa in northern Mozambique (the former site of the frightful impassable rapids named *kebrabassa*, "end of work," by slaves who could proceed no farther upstream). Because the sediment-routing system is strictly partitioned by these two major reservoirs, it is here convenient to distinguish four reaches: (1) an Uppermost Zambezi headwater tract as far as the Kwando confluence, (2) an Upper Zambezi that includes Victoria Falls and the Batoka Gorge as far as Lake Kariba, (3) a Middle Zambezi between the two reservoirs, and (4) a Lower Zambezi downstream of Lake Cahora Bassa (fig. 3).

Sourced among low ridges of the Kasai Shield in the Mwinilunga District of northernmost Zambia and undecided at first whether to head toward the Atlantic or Indian Ocean, the Uppermost Zambezi cuts across Precambrian basement in easternmost Angola. Back to Zambia, the river traverses unconsolidated Kalahari sands and widens in a ~180-km-long floodplain reaching 30 km in width during peak flood (O'Connor and Thomas 1999).

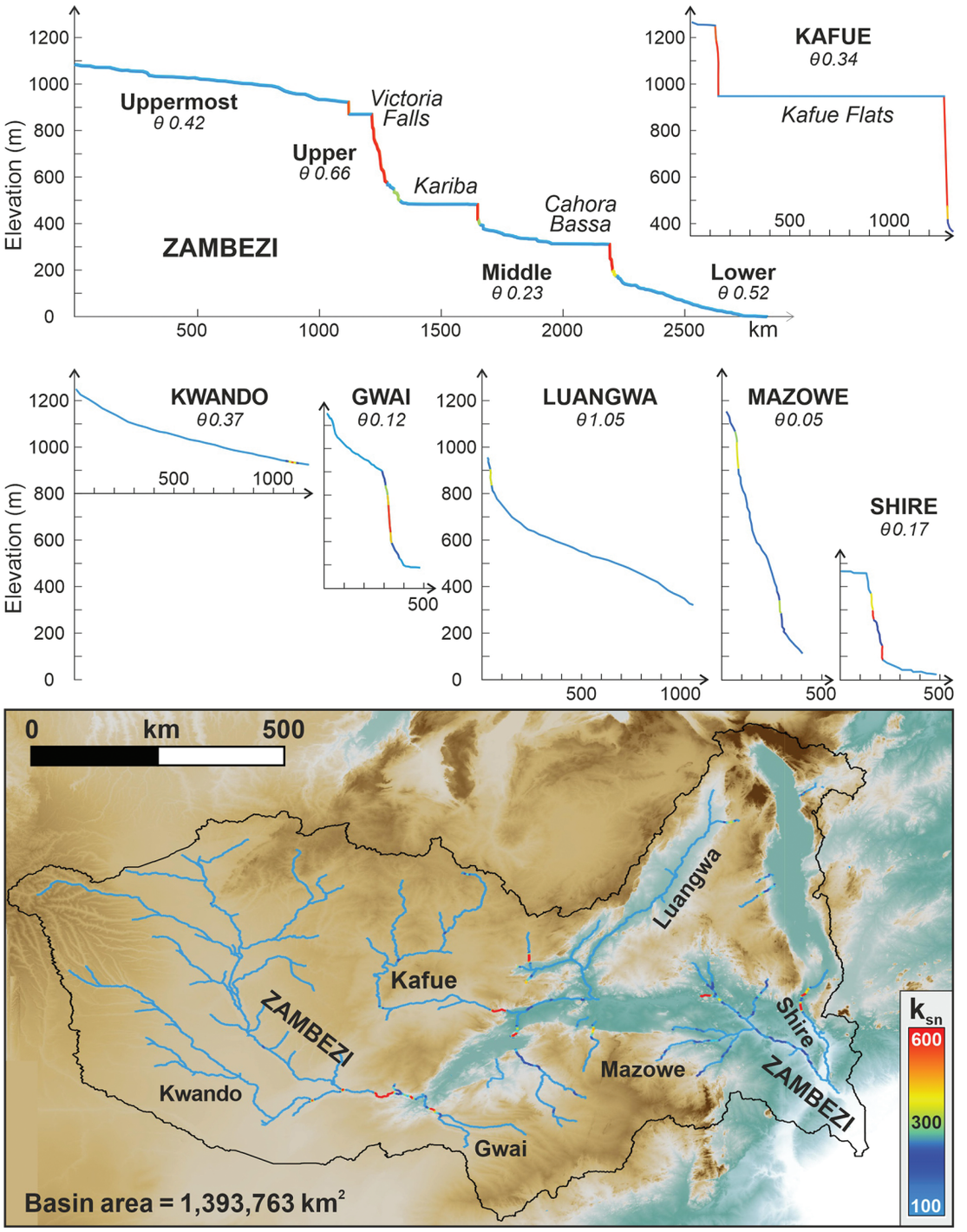

Figure 3. River morphometry (same vertical scale for all profiles; same horizontal scale for tributaries). Besides the concave equilibrium profile of the Kwando, longitudinal channels are highly irregular, as highlighted by extreme variations in both steepness and concavity indices k_{sn} and θ. As with most rivers in southern Africa, the Zambezi and several tributaries (e.g., Gwai, Kafue, Shire) display youthful, staircase profiles with long flat segments separated by very steep tracts, reflecting the presence of stepped planation surfaces separated by escarpments, a characteristic feature of southern African landscape (Knight and Grab 2018).

Tree growth is inhibited by the persistently high water table, and river waters slowly filter through the wetland, where clay accumulates in soils enriched in humus.

The major Uppermost Zambezi tributary is the Kwando River. Sourced in humid Angola, which receives an annual precipitation up to 1400 mm concentrated between December and March, when the southward migration of the Congo Air Boundary brings heavy rains, the river chiefly drains the vegetated Mega-Kalahari dune field (Shaw and Goudie 2002). After entering the Okavango Rift (Modisi et al. 2000; Kinabo et al. 2007), the Kwando (here named Linyanti, and next Chobe) deviates sharply eastward along the Linyanti and Chobe Faults, forming a tectonic depression that favored the recent capture of the Kwando by the Zambezi and is currently favoring the capture of Okavango waters as well, conveyed eastward along the Selinda spillway (Gumbricht et al. 2001). The depression, hosting large swamps and once large paleolakes (Shaw and Thomas 1988), continues into Zambia, where it includes the low-gradient Kasaya and Ngwezi Rivers. These west-bank tributaries of the Zambezi, as the Kabombo (Kabompo) to the north, are sourced in the Lufilian Arc.

Downstream of the Kwando confluence, the Upper Zambezi and its local tributaries (e.g., Sinde from Zambia) incise into Karoo basaltic lavas, where the gradient steepens, forming local rapids. Suddenly, the river plunges some 100 m along the 1.7-km length of the Victoria Falls (in Lozi language *Mosy-wa-Tunya*, "the-Smoke-that-Thunders"), and the turbulent waters downstream carve an amazing zigzag into the deep Batoka Gorge of black Karoo basalt, the result of progressive retreat of the waterfalls during the Quaternary (Derricourt 1976). After receiving tributaries draining Karoo lavas overlain by a veneer of Kalahari dune sand (Masuie and Matetsi from Zimbabwe), the river reaches Lake Kariba shortly downstream of the confluence with the Gwai River. The senile low-gradient upper reaches of this major tributary sourced in the Zimbabwe Craton are incised, as its east-bank subtributaries, in Karoo basalt and sedimentary rocks surrounded by Kalahari dune sand (Thomas and Shaw 1988; Moore et al. 2009*b*), whereas the youthful lower reaches cut steeply across the Paleoproterozoic basement of the Magondi Belt (fig. 3).

In the lower 1400 km, the Zambezi skirts around the Zimbabwe Craton, flowing through a rift zone formed on top of the Pan-African (Kuunga) suture zone (Goscombe et al. 2020) and hosting a thick infill of Karoo sediments and lavas (Nyambe and Utting 1997). The major north-bank Zambian tributaries of the Middle Zambezi are the Kafue and the Luangwa Rivers. The Kafue drains southward into the Lufilian Arc and next turns sharply eastward, cutting across the Zambezi Belt to eventually reach the Zambezi main stem (fig. 3). The Luangwa, sourced in the Ubendian Belt of northernmost Zambia, flows for most of its course along a Karoo rift basin filled with an 8-km-thick Permo-Triassic sedimentary succession (Banks et al. 1995) and finally traverses the Zambezi Belt before joining the Zambezi just upstream of Lake Cahora Bassa.

Major tributaries in Mozambique are the Mazowe (Mazoe) and Luenha (Luia), sourced in the Zimbabwe Craton to the west, and the Shire, the outlet of Lake Malawi (Nyassa). Most detritus contributed by tributaries joining the trunk river from either side is generated from upper Mesoproterozoic gneissic basement reworked during the Neoproterozoic Pan-African orogeny (Grantham et al. 2011). Minor tributaries (e.g., Minjova) and subtributaries in the north also drain the Karoo Supergroup (Fernandes et al. 2015).

Finally, the Lower Zambezi traverses the Cretaceous and Cenozoic sedimentary covers of the Mozambique lowlands (fig. 2). Here the river forms a large floodplain with multiple meandering channels, oxbow lakes, and swamps before emptying into the Indian Ocean, where it feeds a wide shelf extending beyond Beira in the south and Quelimane in the north. The flatness of the shelf, reaching 150 km in width offshore Beira, contributes to the highest tidal range around Africa (up to 6.4 m).

The finest sediment fractions of the river suspended load settle far off the shelf, forming a wide mud apron on the slope between 300- and 2000-m water depth. A considerable fraction of Zambezi sediment, however, is not deposited today offshore of the mouth, but transported toward the northeast, a direction opposite to the mean flow within the Mozambique Strait (Schulz et al. 2011; van der Lubbe et al. 2014). Longshore currents are confined to the inner shelf, whereas the outer shelf is largely covered by palimpsest sand with heavy-mineral lags formed by winnowing by strong oceanic, tidal, and wave-induced currents (Beiersdorf et al. 1980; Miramontes et al. 2020).

The multisourced Zambezi deep-sea fan, one of the Earth's largest turbidite systems active since the Oligocene (Droz and Mougenot 1987), is mainly fed via the ~1200-km-long, curvilinear, and exceptionally wide Zambezi Valley starting at the shelf break offshore Quelimane ~200 km northeast of the Zambezi mouth (fig. 1). In the more than 1000-km-long fan, up to very coarse-grained sand

occurs from the upper canyon to the distal lobes (Kolla et al. 1980; Fierens et al. 2019, 2020).

Drainage Evolution. The history of the Zambezi River reflects the multistep changes of African landscape caused by the progressive breakup of Gondwana (Partridge and Maud 1987; Key et al. 2015; Knight and Grab 2018). Extensional phases in eastern southern Africa started in the Permian (Macgregor 2018). The entire Middle Zambezi and its major tributary the Luangwa River flow along Permo-Triassic rift zones (fig. 2). The eastward slope, instead, originated in the Early Cretaceous by domal uplift related to incipient rifting of the South Atlantic and emplacement of the Paranà-Etendeka large igneous province in the west (Cox 1989; Moore and Blenkinsop 2002). Superposed onto Precambian mobile belts and Permo-Triassic rifts, or intersecting them, the southward propagation of the East African Rift during the Neogene has created further tectonic depressions, including those occupied by Lake Malawi in the east and by the Okavango inland delta in the west (Ebinger and Scholz 2012). The modern Zambezi drainage is thus the result of inheritance from multiple Permo-Mesozoic extensional events on both sides of Africa combined with rifting inside Africa that is still ongoing.

Successive events of river capture and drainage reversal, indicated by sharp changes in direction of its major Kwando, Kafue, and Luangwa tributaries, and the genetic similarities of fish populations between the Kafue and Upper Zambezi and between the Middle Zambezi and the Limpopo, have long suggested that the Zambezi, Okavango, and Limpopo originally formed a single transcontinental river following uplift associated with Early Cretaceous rifting of the South Atlantic (Thomas and Shaw 1988; Moore et al. 2007). In the Paleogene, uplift of the Ovamboland-Kalahari-Zimbabwe axis resulted in endorheic drainage of the Okavango and Upper Zambezi (Moore and Larkin 2001). The then-isolated Lower Zambezi initiated headward erosion, leading to the sequential capture of its middle- and upper-course tributaries. Both Kafue and Luangwa Rivers once drained southwestward, the former joining the Upper Zambezi in the Machili Flats and the latter flowing across the Gwembe trough currently occupied by Lake Kariba (Thomas and Shaw 1991). Linking with the upper course in the Plio-Pleistocene was followed by the capture of the Kwando River, and by the currently occurring capture of the Okavango as well (Wellington 1955; Moore et al. 2007). In northwest Zimbabwe, drainage is largely controlled by an old pre-Karoo surface, tilted westward during domal uplift in the Early Jurassic (Moore et al. 2009*b*). The present east-bank tributaries of the Gwai River all drained westward toward Botswana, until they were captured by headward erosion of the Gwai River after establishment of the modern Zambezi River course (Thomas and Shaw 1988).

Methods

Between 2018 and 2019, we collected 31 sediment samples ranging in size from very fine to coarse sand from active river bars of the Zambezi River and of its major tributaries in Zambia and Mozambique. In 2011, 25 additional sediment samples were collected in the Zambezi, Kwando, and Gwai catchments in Zambia, Caprivi Strip, Botswana, and Zimbabwe. To cover the entire Zambezi system from source to sink, we also studied four fine sands from the Bons Sinais Estuary and adjacent beaches in the Quelimane area of the northern Zambezi delta, and five sandy silts collected offshore of Quelimane (core MOZ4-CS14, 181 m below sea level [b.s.l.]) and of the Zambezi delta (core MOZ4-CS17; 550 m b.s.l.) during the PAMELA-MOZ04 IFREMER-Total survey (Jouet and Deville 2015). Offshore sediments, collected by Calypso piston corer within 25 m below the sea floor, were deposited during the last glacial lowstand (MOZ4-CS17-2402-2407cm, 24.1 ka), the postglacial warming and sea-level rise (MOZ4-CS14-1602-1607cm, 15.9 ka; MOZ4-CS17-702-707cm, 14.6 ka), and the Holocene highstand (MOZ4-CS14-21-26cm, 4.3 ka; MOZ4-CS17-52-57cm, 4.0 ka). These sediments were dated using accelerator mass spectrometer standard radiocarbon methods on marine mollusk shells and bulk assemblages of planktonic foraminifera by applying a local marine reservoir correction of mean $\Delta R = 158 \pm 42$ y. Analyses, calibrated dates, and interpolated age models are illustrated in detail in Zindorf et al. (2021). Full information on sampling sites is provided in table A1 (tables A1–A3 are available online) and Google Earth file Zambezi.kmz (available online).

Petrography. A quartered fraction of each sample was impregnated with Araldite resin, stained with alizarine red to distinguish dolomite and calcite, cut into a standard thin section, and analyzed by counting 400 or 450 points by the Gazzi-Dickinson method (Ingersoll et al. 1984). Sand is classified according to the three main groups of framework components (Q = quartz; F = feldspars; L = lithic fragments), considered where exceeding 10%QFL and listed in order of abundance (classification scheme after Garzanti 2019). Feldspatho-quartzose sand is thus

defined as Q > F > 10%QFL > L, formally distinguishing between feldspar-rich (Q/F < 2) and quartz-rich (Q/F > 4) compositions. Pure quartzose sand is defined as Q/QFL > 95%. These distinctions proved to be essential to discriminate among lithic-poor siliciclastic sediments generated from cratonic blocks and deposited along passive continental margins in different geomorphological settings (Garzanti et al. 2018*b*). Microcline with cross-hatch twinning is called for brevity "microcline" through the text. Median grain size was determined in thin section by ranking and visual comparison with standards of $\phi/4$ classes prepared by sieving in our laboratory.

Heavy Minerals. From a split aliquot of the widest convenient size-window obtained by wet sieving (mainly 15–500 μm), heavy minerals were separated by centrifuging in Na-polytungstate (2.90 g/cm^3) and recovered by partial freezing with liquid nitrogen. In grain mounts, ≥200 transparent heavy minerals for each sample were either grain counted by the area method or point counted at appropriate regular spacing to obtain correct volume percentages (Garzanti and Andò 2019). Mineralogical analyses were carried out by routinely coupling observations under the microscope and the Raman spectroscope. Transparent heavy-mineral assemblages, called for brevity "tHM suites" throughout the text, are defined as the spectrum of detrital extrabasinal minerals with density > 2.90 g/cm^3 identifiable under a transmitted-light microscope. According to the transparent heavy-mineral concentration in the sample (tHMC), tHM suites are defined as extremely poor (tHMC < 0.1), very poor (0.1 ≤ tHMC < 0.5), poor (0.5 ≤ tHMC < 1), moderately poor (1 ≤ tHMC < 2), moderately rich (2 ≤ tHMC < 5), rich (5 ≤ tHMC < 10), very rich (10 ≤ tHMC < 20), or extremely rich (tHMC > 20).

The sum of zircon, tourmaline, and rutile over total transparent heavy minerals (ZTR index of Hubert 1962) expresses the chemical durability of the tHM suite. The "amphibole color index" (ACI) varies from 0 in detritus from greenschist, blueschist, or lowermost amphibolite-facies rocks yielding exclusively blue or blue-green amphibole to 100 in detritus from granulite-facies or volcanic rocks yielding exclusively brown amphibole (Andò et al. 2014).

Significant minerals are listed in order of abundance (high to low) throughout the text. Key compositional parameters are summarized in table 1. The complete petrographic and heavy-mineral data sets are provided in tables A2 and A3.

River Morphometry. The geomorphological properties of the Zambezi River and its major tributaries were quantified using TopoToolbox, a set of MATLAB functions for the analysis of relief and flow pathways in digital elevation models (DEM; Schwanghart and Scherler 2014). The analysis of the longitudinal profile of bedrock channels was carried out on a 90-m-resolution DEM provided by Shuttle Radar Topography Mission Global (SRTM GL3; https://opentopography.org) to identify major knickpoints, defined as sites where the channel gradient changes abruptly owing to sharp local changes in bedrock strength and/or uplift rate.

Channel concavity θ and normalized channel-steepness k_{sn} (referenced to a fixed concavity 0.45 to facilitate comparison among channel slopes with widely varying drainage areas and concavities) are defined by the power-law relationship $S = k_s A^{-\theta}$ between the local channel slope S and the contributing drainage area A used as a proxy for discharge (Flint 1974; Whipple 2004).

Data

In the partitioned Zambezi sediment-routing system, sand compositional signatures are radically different upstream and downstream of both Lake Kariba and Lake Cahora Bassa (table 1), indicating that no sand can pass across each reservoir. In the Uppermost Zambezi main stem, as in some of its major tributaries including the Kwando and the Kafue, another factor hampering the continuity of downstream sediment transport is the occurrence of densely vegetated flat lowland occupied by numerous pans commonly aligned with shallow grassy valleys (*dambos*) acting as natural sediment traps (Moore et al. 2007).

The Uppermost Zambezi. Near the source, close to the political boundaries of Zambia, Congo, and Angola, sand is pure quartzose with K-feldspar >> plagioclase and a very poor tHM suite dominated by zircon with tourmaline, minor rutile, and staurolite (fig. 4*A*). Kyanite increases downstream and clinopyroxene is significant upstream of the Kwando confluence.

The Kwando River from Angola contributes pure quartzose sand with a very poor tHM suite including zircon, tourmaline, kyanite, and staurolite (fig. 5*A*). Sand of west-bank tributaries from Zambia ranges from quartz-rich feldspatho-quartzose with K-feldspar > plagioclase (Kabombo, Ngwezi) to pure quartzose with K-feldspar >> plagioclase (Kasaya). Muscovite occurs. The tHM suites vary from poor with tourmaline, rutile, epidote, and kyanite (Kabombo) to very poor and including epidote, zircon, tourmaline, staurolite, and green augite (Kasaya), or epidote dominated with amphibole and minor garnet (Ngwezi).

Table 1. Key Petrographic and Heavy-Mineral Signatures

River	No.	Q	F	Lvm	Lsm	Lmfb	QFL total	P/F (%)	Mica (%)	tHMC	ZTR	Ap	Ttn	Ep	Grt	St	Ky	Sil	Amp	Cpx	Hyp	&tHM	HM total	ACI
Kwando River	3	99	1	0	0	0	100.0	n.d.	0	.1	61	.3	.3	3	0	16	16	0	2	0	0	1	100.0	39
Ust. Z. tributaries	3	90	9	.2	.5	0	100.0	36	2	.4	31	1	1	38	2	5	6	1	7	5	2	2	100.0	0–5
Uppermost Zambezi	**6**	**96**	**3**	**0**	**0**	**0**	100.0	**32**	**.1**	**.4**	**60**	**0**	**.4**	**5**	**.3**	**7**	**18**	**0**	**2**	**4**	**0**	**2**	100.0	**0**
U.Z. tributaries pre-VF	1	91	1	7	1	0	100.0	n.d.	0	.3	5	.4	0	.4	0	1	0	0	.4	92	0	0	100.0	n.d.
Upper Zambezi pre-VF	**4**	**96**	**2**	**1**	**0**	**.2**	100.0	**47**	**0**	**.4**	**34**	**0**	**0**	**8**	**.2**	**3**	**23**	**.5**	**3**	**27**	**0**	**1**	100.0	**0–39**
U.Z. tributaries pre-K	2	46	2	52	0	0	100.0	n.d.	0	10.5	0	0	0	3	0	0	0	0	0	97	0	0	100.0	n.d.
Upper Zambezi pre-K	**4**	**93**	**3**	**4**	**0**	**0**	100.0	**60**	**0**	**1.3**	**3**	**.3**	**0**	**2**	**.2**	**2**	**6**	**0**	**1**	**84**	**0**	**1**	100.0	n.d.
Gwai River	3	74	22	3	1	1	100.0	61	4	1.6	3	1	0	18	7	.3	1	1	35	30	.2	1	100.0	11–37
Gwai tributaries	5	83	11	5	.5	0	100.0	60	0	3.5	12	1	2	27	2	1	.2	0	12	43	0	.4	100.0	8–34
Kafue	2	67	29	.4	.5	3	100.0	41	6	6.7	8	2	3	10	2	1	4	1	67	1	0	1	100.0	9–16
Middle Zambezi	**2**	**63**	**32**	**1**	**2**	**2**	100.0	**36**	**4**	**4.8**	**12**	**1**	**4**	**14**	**2**	**0**	**6**	**.2**	**51**	**6**	**1**	**2**	100.0	**9–16**
Luangwa	1	74	25	0	0	1	100.0	39	.3	2.9	11	1	4	18	6	4	11	7	35	1	0	2	100.0	46
Sangara-Chacangara	2	49	48	.3	3	.5	100.0	44	.1	3.2	4	2	.2	4	3	0	1	0	20	41	21	4	100.0	13–24
Morrunguze	1	46	50	0	1	4	100.0	51	1	14.7	2	1	3	12	4	0	0	0	30	36	12	0	100.0	41
Minjova	1	70	26	1	3	0	100.0	55	0	.4	6	1	1	7	25	0	0	.5	26	24	9	.5	100.0	91
Mufa	2	47	50	1	1	.2	100.0	44	1	12.1	2	2	3	2	2	0	.5	0	71	9	8	1	100.0	45–50
Mazowe-Luenha	2	45	53	1	0	1	100.0	38	1	9.0	3	1	4	12	3	0	2	1	73	1	.5	0	100.0	31–38
Lower Zambezi	**2**	**48**	**50**	**1**	**.4**	**.2**	100.0	**58**	**5**	**16.4**	**5**	**1**	**1**	**9**	**25**	**0**	**.2**	**.5**	**43**	**7**	**5**	**2**	100.0	**14–63**
Shire	1	33	67	0	0	.4	100.0	72	3	14.1	4	4	.4	6	4	0	1	0	76	2	2	0	100.0	41
Sangadze-Zangue	2	64	35	0	1	.2	100.0	28	0	1.2	2	2	1	5	58	7	4	3	18	1	.2	.5	100.0	27–80
Lower Zambezi (final)	**2**	**49**	**49**	**1**	**0**	**1**	100.0	**45**	**3**	**6.9**	**3**	**1**	**4**	**21**	**3**	**2**	**1**	**.2**	**58**	**3**	**3**	**0**	100.0	**26–38**
Zambezi upper slope	3	63	35	.2	1	1	100.0	52	11	3.1	4	2	4	23	3	.2	1	3	46	11	2	1	100.0	4–7
Quelimane coast	4	69	28	1	2	.4	100.0	53	2	4.5	5	2	4	17	4	.5	1	2	53	8	3	.2	100.0	2–11
Quelimane outer shelf	2	58	40	1	1	.5	100.0	46	29	2.2	5	3	2	24	.2	0	.2	4	47	14	1	1	100.0	4–8

Note. Q = quartz; F = feldspars (P = plagioclase); L = lithic grains (Lvm = volcanic to low-rank metavolcanic; Lsm = sedimentary to low-rank metasedimentary; Lmfb = high-rank felsic metamorphic and metabasite); tHMC = transparent heavy-mineral concentration; ZTR = zircon + tourmaline + rutile; Ap = apatite; Ttn = titanite; Ep = epidote; Grt = garnet; St = staurolite; K = Lake Kariba; Ky = kyanite; Sil = sillimanite; Amp = amphibole; Cpx = clinopyroxene; Hyp = hypersthene; &tHM = other transparent heavy minerals (mainly anatase and andalusite with monazite, olivine, or enstatite locally); ACI = amphibole color index; n.d. = not determined; Ust. Z. = Uppermost Zambezi; U.Z. = Upper Zambezi; VF = Victoria Falls. Boldface indicates Zambezi main stem.

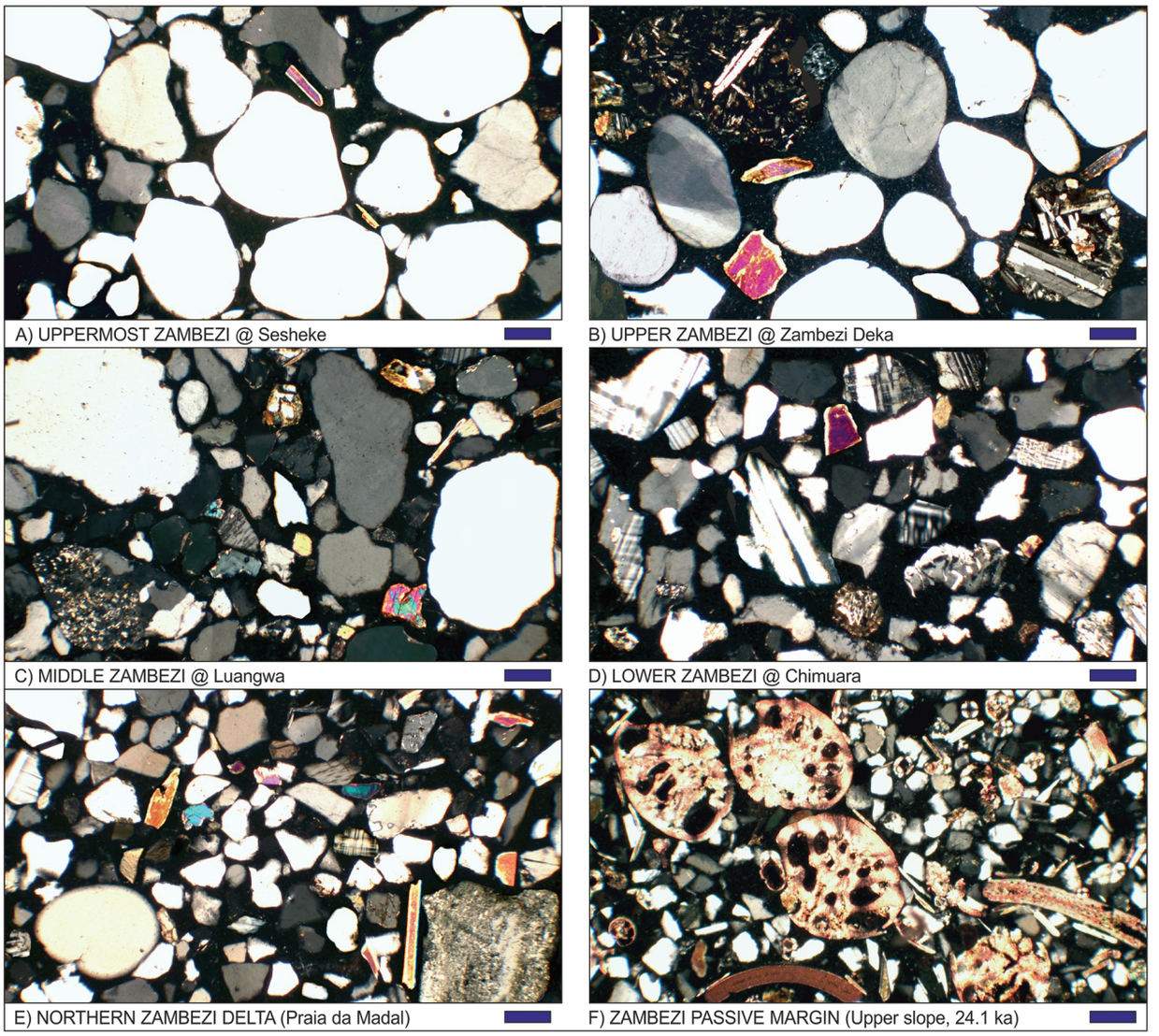

Figure 4. Petrographic changes along Zambezi sediment-routing system from source to sink. *A*, Pure quartzose sand recycled from the Mega-Kalahari Desert. *B*, Marked enrichment in lathwork to microlitic volcanic rock fragments and clinopyroxene in quartzose sand downstream of Victoria Falls. *C*, Reconstituted feldspatho-quartzose metamorphiclastic bedload downstream of Lake Kariba. *D*, Sharp increase in feldspars in reconstituted bedload downstream of Lake Cahora Bassa. *E*, Feldspatho-quartzose beach sand in the Quelimane area. *F*, Very fine-grained feldspar-rich feldspatho-quartzose sand containing benthic foraminifera (stained by alizarine red) and deposited during the last glacial lowstand on the upper slope offshore of the Zambezi mouth. All photos with crossed polars; blue bar for scale = 100 μm.

The Upper Zambezi. Basaltic detritus from Karoo lavas mixes with quartz as the river approaches Victoria Falls, and in steadily increasing proportions across the gorges downstream of the falls. Upstream of Lake Kariba, bedload sand and levee silty sand include mafic volcanic rock fragments with lathwork and microlitic textures (fig. 4*B*) and are, respectively, quartzose with plagioclase ≈ K-feldspar and litho-feldspatho-quartzose with plagioclase >> K-feldspar. The moderately rich tHM suite consists almost entirely of green augite with a few olivine grains.

Upstream of Victoria Falls, the Sinde tributary from Zambia carries quartzose sand with mafic

Figure 5. Sand composition in major Zambezi tributaries. *A*, Up to well-rounded monocrystalline quartz grains recycled from Mega-Kalahari dunes. *B*, High-rank metamorphic rock fragments and microcline derived first-cycle from the Magondi Belt. *C*, Biotite-rich metamorphic detritus from the Lufilian Arc and Zambezi Belt mixed with rounded recycled quartz. *D*, Deeply corroded quartz and feldspar grains derived from the Irumide Belt and recycled from Karoo strata. *E*, Abundant microcline with high-rank metamorphic rock fragments from the Archean Zimbabwe Craton and Proterozoic gneisses. *F*, Microcline, gabbroic rock fragments, pyroxene, and amphibole from the southern Irumide Belt and Tete gabbro-anorthosite complex. *G*, Dominant feldspar derived from orthogneisses and granulites of the Blantyre domain. *H*, Skeletal quartz and weathered K-feldspar grains in Mozambican lowlands. All photos with crossed polars; blue bar for scale = 100 μm.

volcanic grains and a poor tHM suite dominated by brown and green augite. Basaltic detritus increases in tributary sand downstream of the falls. Masuie and Matetsi sands are, respectively, lithic-rich litho-quartzose and quartzo-lithic basalticlastic, with rich and very rich tHM suites consisting almost exclusively of augite and augite-bearing rock fragments.

River bars and levees of the Gwai River from Zimbabwe consist of feldspatho-quartzose sand with plagioclase > K-feldspar (fig. 5*B*). Mostly biotitic mica is concentrated in levee silty sand. The moderately rich tHM suite consists of amphibole with subordinate epidote, garnet, and clinopyroxene. The Deka River carries quartz-rich litho-quartzose basalticlastic sand with a very rich tHM suite dominated by clinopyroxene with some epidote.

The Middle Zambezi. Downstream of Lake Kariba, Zambezi sand has the same feldspar-rich feldspatho-quartzose composition as Kafue River sand, with K-feldspar >> plagioclase, some metamorphic rock fragments, and micas (biotite ≥ muscovite; figs. 4*C* and 5*C*). The rich tHM suite includes amphibole (blue-green to green-brown hornblende and actinolite) and subordinate epidote, kyanite, and clinopyroxene. Amphibole decreases and zircon increases slightly downstream on the main stem.

The Luangwa River carries feldspatho-quartzose sand with K-feldspar >> plagioclase and granitoid to gneissic rock fragments, with a moderately rich tHM suite including mainly amphibole (green-brown to blue-green hornblende), kyanite, zircon, and prismatic or fibrolitic sillimanite (fig. 5*D*).

The Lower Zambezi. In Mozambique, Zambezi sand ranges from quartzo-feldspathic to feldspar-rich feldspatho-quartzose with K-feldspar ≥ plagioclase (fig. 4*D*). Mica (mostly biotite) is common in very fine sand. The rich tHM suite includes mostly amphibole (blue-green to green-brown hornblende and actinolite), subordinate epidote, locally strongly enriched garnet, and minor titanite, zircon, clinopyroxene, and hypersthene.

Most tributaries contribute quartzo-feldspathic sand with K-feldspar ≥ plagioclase and a rich tHM suite (figs. 5*E*–5*G*). An exception is represented by the Minjova and Zangue tributaries, which carry feldspatho-quartzose and quartz-rich feldspatho-quartzose sand with a poor tHM suite (fig. 5*H*). Feldspars (mostly plagioclase) are twice as abundant as quartz in Shire sand from Malawi. Metabasite grains are significant in Morrunguze sand (fig. 5*F*). Chacangara sand includes gabbroic, quartzose sandstone/metasandstone, and shale/slate rock fragments.

The tHM suites are diverse. Amphibole (mainly green-brown and blue-green hornblende) is dominant in Mufa, Mazowe, Luenha, and Shire sand (ACI 31–50), and common in most other tributaries (ACI 13–27 in Sangara, Chacangara, and Zangue sand but up to 80–91 in Sangadze and Minjova sand). Clinopyroxene and hypersthene are most abundant in Chacangara sand and also characterize Sangara, Morrunguze, Minjova, and, to a lesser extent, Mufa sand (table 1). Epidote is invariably present in moderate amounts. Garnet is dominant in Sangadze sand and common in Zangue and Minjova sand. Staurolite is associated with kyanite and prismatic or fibrolitic sillimanite in Zangue sand. Kyanite and sillimanite also occur in Luenha sand. Zircon and other durable minerals, as well as titanite and apatite, are minor (ZTR up to eight in Sangara sand). Rare olivine was detected in Sangara, Chacangara, and Mufa sands.

The Northern Coast, the Shelf, and the Slope. Sand in the Bons Sinais Estuary near Quelimane and adjacent beaches, located between 100 and 130 km north of the Zambezi mouth, is feldspatho-quartzose with plagioclase ≥ K-feldspar and a rich tHM suite including mainly blue-green amphibole, subordinate epidote, clinopyroxene, and minor titanite, garnet, hypersthene, and mostly prismatic sillimanite (fig. 4*E*).

Very fine-grained sand to coarse silt, cored on the upper continental slope ~85 km offshore of the Zambezi delta and close to the shelf break ~80 km to the east-northeast of the Bons Sinais mouth, is feldspar-rich feldspatho-quartzose with K-feldspar ≈ plagioclase and a moderately rich tHM suite including blue-green amphibole, epidote, clinopyroxene, and minor prismatic sillimanite, titanite, tourmaline, apatite, hypersthene, and garnet. Benthic foraminifera are abundant (fig. 4*F*). No major mineralogical difference is observed either between samples cored offshore of the Zambezi mouth and Quelimane area or among sediments deposited during the last glacial lowstand, the postglacial sea-level transition, and the Holocene highstand in both areas.

Sand Generation in the Zambezi Catchment

The Uppermost Zambezi: Polycyclic Sand from the Kalahari. Sand generated in southeastern Angola and westernmost Zambia and carried by the Uppermost Zambezi and its Kwando tributary consists almost entirely of monocrystalline quartz with very poor, ZTR-dominated tHM suite including staurolite and kyanite, a mineralogical signature that reflects extensive recycling of Kalahari desert sand (figs. 6 and 7). The sedimentary succession of this vast rim basin, formed on the low-relief

southern Africa plateau confined between the rejuvenated shoulders of the Indian and Atlantic rifted margins, is largely of fluvial origin with secondary eolian imprint (Moore and Dingle 1998). Kalahari dunes are generally best developed west of river channels, suggesting deflation of fluvial sediments by easterly winds during drier periods (Shaw and Goudie 2002). Conversely, rivers have inundated interdune areas and incised their course across dune ridges during wetter periods (Thomas et al. 2000). Between a fourth and a half of quartz grains are well rounded in both dune and river sediments, indicating that climate-controlled cycling of quartz-rich sand has taken place repeatedly from the fluvial to the eolian environment and back (Thomas and Shaw 2002).

The Upper Zambezi: Mixing with Detritus from Karoo Basalts. The Zambezi first meets Karoo basalt at Ngonye Falls in southwest Zambia and from there on the river flows along Karoo rift basins as far as the Mozambican lowlands. Pure quartzose sand recycled from the Kalahari mixes downstream with detritus derived locally from Lower Jurassic Karoo basalt in increasing proportions, determined accurately with forward-mixing models based on integrated petrographic and heavy-mineral data (Garzanti et al. 2012; Resentini et al. 2017).

Although the sand generation potential of basalt is notably less than that of sandstone or granite (Garzanti et al. 2019*b*, 2021*b*, 2021*c*; Le Pera and Morrone 2020; Morrone et al. 2020), mafic lava contains and sheds much more clinopyroxene than the few heavy minerals that quartzose sandstone contains and can thus supply. Therefore, wherever basaltic detritus mixes with recycled quartz, as in the Upper Zambezi, quartz still dominates among main framework grains but the tHM suite rapidly becomes clinopyroxene dominated (figs. 6 and 7). From upstream of Victoria Falls to the Batoka Gorge, basaltic detritus accounts for <3% of total sediment only and Upper Zambezi sand remains pure quartzose, although clinopyroxene steadily increases from 14% to 86% of the very poor to poor tHM suite. Basaltic detritus increases to ~12% upstream of Lake Kariba, with composition changed to quartzose with 9% basaltic rock fragments in bedload sand and to litho-feldspatho-quartzose in levee silty sand. Clinopyroxene represents 95% and 90% of the moderately rich and rich tHM suite, respectively.

Among Upper Zambezi tributaries, basaltic detritus represents ~10% of Sinde sand in Zambia, and ~15% of Shangani sand, 50% of Masuie sand, and up to 70% of Matetsi sand in Zimbabwe, the rest being mostly represented by quartz recycled from Kalahari dunes. Clinopyroxene invariably represents >90% of the tHM suite in these rivers.

Such estimates are corroborated by clay-mineral and geochemical data, displaying an increase in

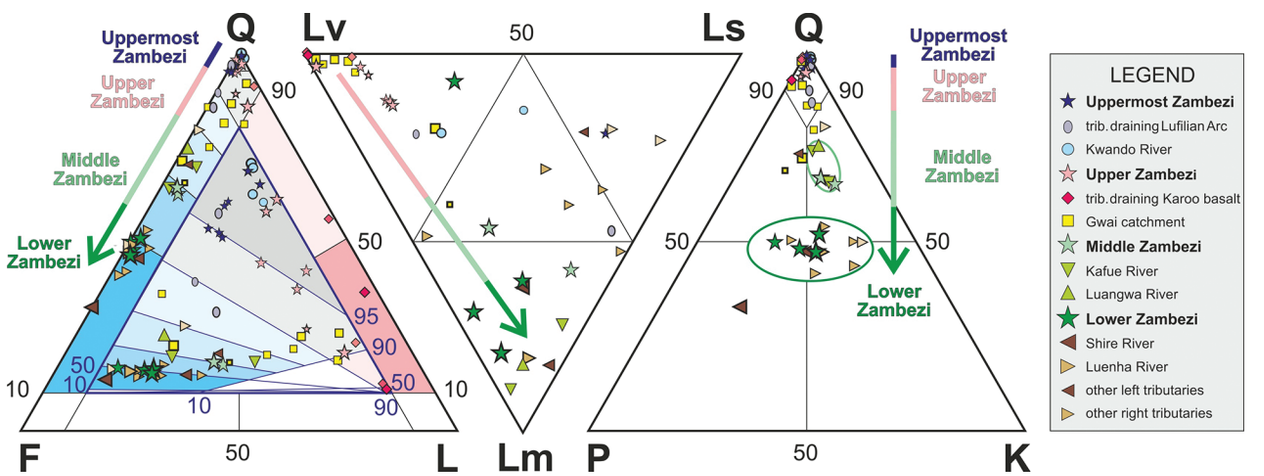

Figure 6. Downstream quartz decrease along segmented Zambezi sediment-routing system. Composition changes stepwise from pure quartzose (Uppermost Zambezi) to quartzose volcaniclastic (Upper Zambezi), feldspar-rich feldspatho-quartzose (Middle Zambezi), and finally quartzo-feldspathic metamorphiclastic (Lower Zambezi). Symbol size is roughly proportional to tributary (trib.) size and increases downstream along the main stem. Smaller symbols with thicker outline are Upper Zambezi and Gwai River levee samples representing deep suspended load. Q = quartz; F = feldspars (P = plagioclase; K = K-feldspar); L = lithics (Lm = metamorphic; Lv = volcanic; Ls = sedimentary). Fields in the QFL diagram after Garzanti (2019); in the nested blue version of the same QFL plot, data are centered to allow better visualization of quartz-rich samples (von Eynatten et al. 2002).

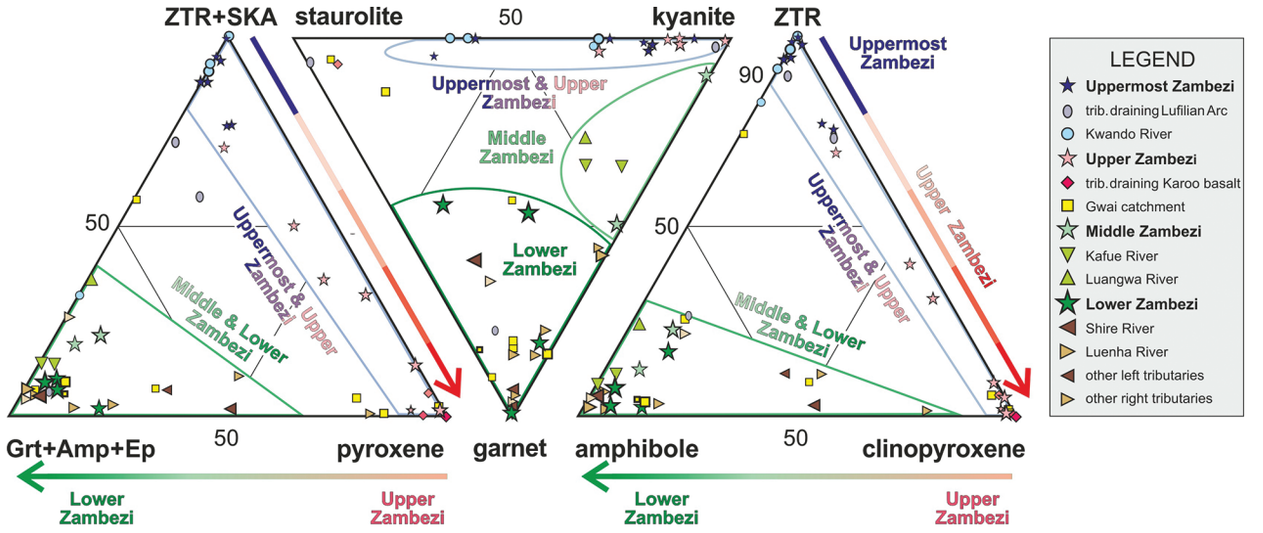

Figure 7. Changes in transparent heavy-mineral suites downstream on the segmented Zambezi sediment-routing system. Note (1) dominance of durable ZTR (zircon, tourmaline, and rutile) and SKA (staurolite, kyanite, sillimanite, and andalusite) minerals in the Uppermost Zambezi; (2) progressive increase in clinopyroxene along the Upper Zambezi; and (3) sharp increase in basement-derived garnet (Grt), amphibole (Amp), and epidote (Ep) in the Middle and Lower Zambezi. Scarcity of garnet in Uppermost and Upper Zambezi sand is ascribed to high weatherability inherited from past hot-humid subequatorial climate. Symbol size is roughly proportional to tributary (trib.) size and increases downstream along the main stem. Smaller symbols with thicker outline are Upper Zambezi and Gwai River levee samples representing deep suspended load.

smectite and in the concentration of Fe, Mg, Ca, Na, Sr, Ti, Eu, V, Cr, Mn, Co, Ni, Cu, and P along the Upper Zambezi, whereas the $^{87}Sr/^{86}Sr$ and weathering indices decrease, $\varepsilon Nd_{(0)}$ becomes only moderately negative, and T_{DM} model ages younger (Garzanti et al. 2014*a*). Forward-mixing calculations based on the integrated geochemical data set indicate that volcanic detritus increases from ~1% for sand and ~14% for cohesive (<32 μm) mud upstream of Victoria Falls up to 17%–18% for sand, 19%–20% for sandy silt, and ~41% for cohesive mud upstream of Lake Kariba. These estimates imply that up to ~27% of the sand and ~45% of the mud that the Upper Zambezi carries toward Lake Kariba is generated downstream of Victoria Falls, from basaltic rocks of the Batoka Gorge and supplied by tributaries draining Karoo lavas and overlying Kalahari dunes.

The Middle Zambezi: First-Cycle and Recycled Detritus from Zambia. The Middle Zambezi flows along Karoo extensional troughs (fig. 2). These formed on top of the Kuunga suture zone, marking the boundary between the Zimbabwe-Kalahari and Congo cratonic blocks and sealed during the final stages of the Neoproterozoic Pan-African orogeny (Goscombe et al. 2020).

The first major tributary joining the Zambezi ~70 km downstream of Lake Kariba is the Kafue River, which largely drains mid-Neoproterozoic volcano-sedimentary rocks and upper Tonian granites of the Lufilian Arc in the upper course. In the lowermost course, the Kafue cuts across the West Zambezi Belt, including polymetamorphic basement of the Congo Craton deformed at upper-amphibolite-facies conditions around 675 Ma (fig. 6 in Goscombe et al. 2020).

Because sand cannot pass Lake Kariba, Middle Zambezi sand downstream of the Kafue confluence acquires the same feldspar-rich feldspathoquartzose metamorphiclastic signature of Kafue sand—with a little more siltstone/sandstone rock fragments and clinopyroxene derived locally from the Karoo Supergroup—which is maintained as far as the confluence with the Luangwa River near the entry point into Lake Cahora Bassa (fig. 8).

The Luangwa River, sourced in Paleoproterozoic gneisses of the Ubendian Belt, follows for most of its course another arm of the Karoo rift network. The Luangwa rift is bordered to the north by the external nappes of the Irumide Belt, including Paleoproterozoic granitoid gneiss overlain by quartzite and schist of the Muva Supergroup deformed at greenschist to amphibolite facies at 1.05–1.02 Ga (De Waele et al. 2009). Exposed to the south is the high-grade internal zone of the southern Irumide Province (fig. 7 in Goscombe et al. 2020). Luangwa

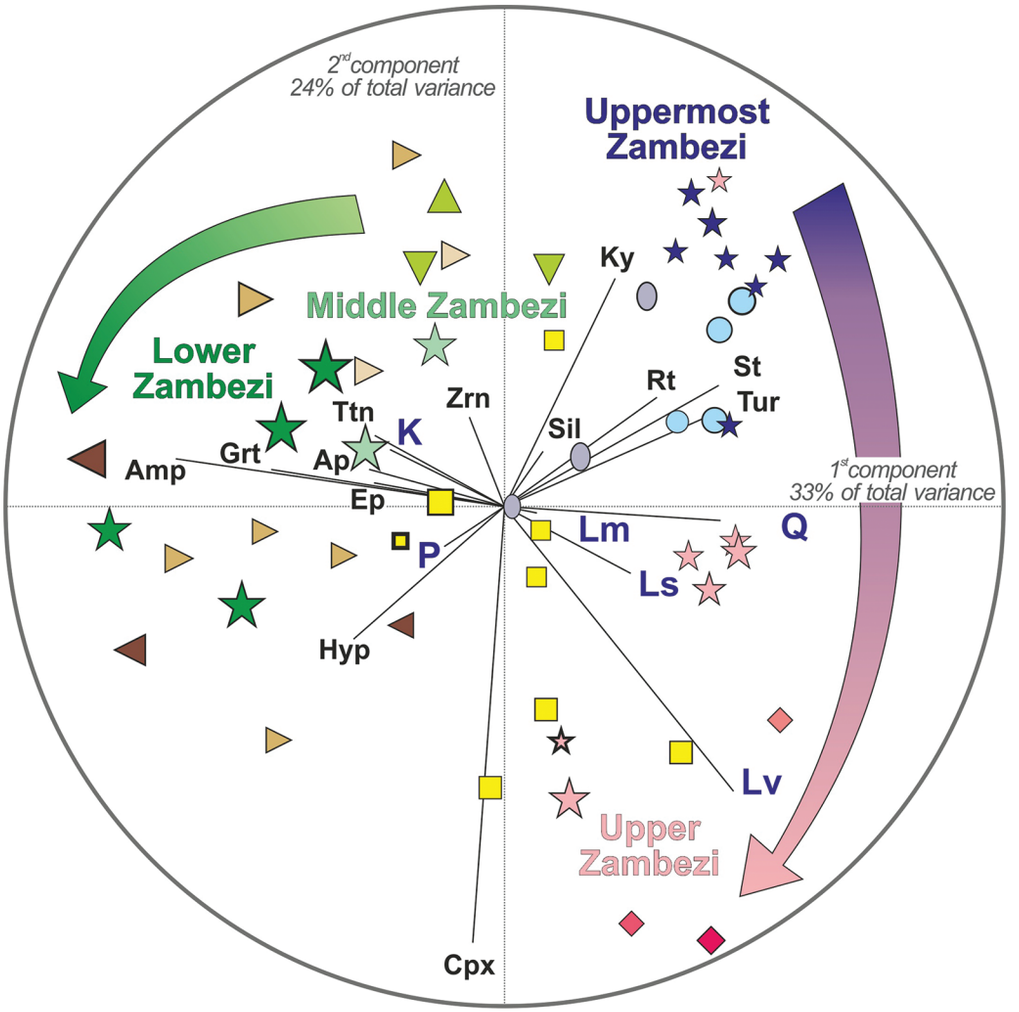

Figure 8. Stepwise changes in compositional signatures along segmented Zambezi sediment-routing system. Pure quartzose sand in the Uppermost Zambezi and Kwando Rivers is progressively enriched in clinopyroxene and basaltic rock fragments downstream in the Upper Zambezi. Middle Zambezi sand chiefly reflects contribution from the Kafue River. Lower Zambezi sand is markedly enriched in feldspars, amphibole, and garnet largely derived from Irumide Belts strongly affected by the Pan-African orogeny. The biplot (Gabriel 1971) displays multivariate observations (points) and variables (rays). The length of each ray is proportional to the variance of the corresponding variable; if the angle between two rays is 0°, 90°, or 180°, then the corresponding variables are perfectly correlated, uncorrelated, or anticorrelated, respectively. Ap = apatite; Hyp = hypersthene; Ky = kyanite; Rt = rutile; Sil = sillimanite; St = staurolite; Ttn = titanite; Tur = tourmaline; Zrn = zircon. Other symbols as in figures 6 and 7.

sand is thus a mixture of detritus derived from up to high-grade metamorphic rocks and recycled from Carboniferous to Jurassic siliciclastic strata, as indicated by relatively high quartz and ZTR minerals coexisting with blue-green to brown hornblende and mainly prismatic sillimanite.

The Lower Zambezi: Feldspar-Rich Sand from Precambrian Basements. As Upper Zambezi sand is dumped into Lake Kariba, Middle Zambezi sand is stored in Lake Cahora Bassa. Composition changes therefore again in the Lower Zambezi, where sand supplied by tributaries largely draining felsic to mafic igneous and up to high-grade metamorphic rocks acquires a quartzo-feldspathic signature unique among the Earth's big rivers (Potter 1978; Garzanti 2019). Most Lower Zambezi tributaries carry sand with Q/F ratio ≤ 1 (fig. 6), reflecting mostly first-cycle provenance from midcrustal crystalline basements. Detritus recycled from the sedimentary fill of Karoo, Cretaceous, or Cenozoic

extensional basins is widespread, although subordinate. This is revealed by sandstone and shale rock fragments in Chacangara sand and by a higher Q/F ratio and poor tHM suite in sand of the Zangue River draining the northern edge of the Urema Graben and of the Minjova River draining the Karoo Moatize-Minjova Basin (Fernandes et al. 2015).

The Sangara, Chacangara, and Mufa west-bank tributaries and the Morrunguze and Minjova east-bank tributaries drain high-grade rocks of the internal zone of the southern Irumide Province, including the Tete gabbro-anorthosite complex (fig. 1 in Goscombe et al. 2020). This is reflected by the occurrence of gabbroic or metabasite rock fragments and by up to very rich tHM suites including hypersthene and clinopyroxene, brown hornblende, and rare olivine.

The Luenha-Mazowe river system drains well into the Archean Zimbabwe Craton in the upper course and cuts downstream across the polymetamorphic Mudzi migmatitic gneisses remobilized during the Pan-African orogeny, and next across the Neoproterozoic Marginal Gneiss. The mostly first-cycle origin of their quartzo-feldspathic sand is reflected by the rich amphibole-dominated tHM suite, as in Mufa sand to the north (fig. 7).

The lowest Q/F ratio is recorded in Shire sand, also including a very rich, amphibole-dominated tHM suite derived from granitic orthogneisses of the Blantyre domain (southern Malawi-Unango Complex), where Stenian-age crust underwent granulite-facies metamorphism during the Pan-African orogeny (Goscombe et al. 2020).

The Sangadze and Zangue lowermost-course tributaries are sourced in the Pan-African Umkondo Belt, including greenschist facies to lower-amphibolite-facies schists thrust onto the margin of the Zimbabwe Craton and upper-amphibolite-facies migmatitic gneisses in the core, whereas the lower course cuts across the Cretaceous to Cenozoic sediment fill of the Lower Zambezi graben. Recycling is manifested in Zangue sand by the highest Q/F ratio of all Lower Zambezi tributaries. Poor to moderately poor, garnet-dominated (Sangadze) or garnet-staurolite (Zangue) tHM suites reflect both first-cycle provenance from lower-amphibolite-facies metasediments of the Umkondo Belt and recycling of Cretaceous sandstones derived from them (e.g., Sena Formation; Salman and Abdula 1995). The occurrence of brown amphibole and prismatic sillimanite, instead, reveals minor but significant contribution from upper-amphibolite-facies to granulite-facies gneisses of the orogen's core (e.g., Stenian Barue Complex; fig. 1 in Goscombe et al. 2020).

Forward-mixing models based on integrated petrographic and heavy-mineral data suggest that most Lower Zambezi sand (60%–80%) is generated in subequal proportions in the Luenha-Mazowe river system sourced in the Zimbabwe Craton and in the trunk-river catchment upstream of the Luenha confluence, including the Zambezi Belt and the southern Irumide Province. Additional contributions from the Umkondo Belt and recycled from the Karoo, Cretaceous, or Cenozoic extensional basins drained by the Minjova, Sangadze, and Zangue tributaries are significant (~20%), whereas supply from the Tete gabbro-anorthosite complex and Blantyre domain, drained respectively by the Morrunguze and Shire tributaries, appears to be subordinate (~10%).

The Zambezi Passive Margin. Detrital modes of Lower Zambezi sand match neither those of estuary and beach sands in the northern delta near Quelimane nor sediments cored offshore of both the Zambezi mouth and Quelimane area and deposited during either the Holocene highstand or the previous postglacial and glacial relative lowstands (table 1). The Q/F ratio is 1.0 ± 0.1 in Lower Zambezi sand but 2.5 ± 0.5 in sand of the Quelimane area and 1.6 ± 0.3 in offshore samples. The homogeneous composition of offshore sediments generated before the mid-Holocene (older than 4 ka) suggests that this could represent the original, pre-Anthropocene signature of Zambezi sediment.

Subsequent closure of the Kariba and Cahora Bassa dams—with consequent drastic reduction of the catchment area effectively contributing sediment to the Zambezi delta—explains the peculiar mineralogical signatures characterizing Lower Zambezi sand today. Besides the abundance of feldspars, these include the high tHMC and ACI indices, reflecting provenance dominantly from middle-crustal igneous and high-grade metamorphic rocks. The abundance of mica in offshore sediments, instead, is the effect of preferential winnowing of slow-settling platy phyllosilicates by waves, a phenomenon observed along continental shelves worldwide (e.g., Doyle et al. 1968; Garzanti et al. 2015, 2019*a*).

The mineralogy of estuary and beach sand in the Quelimane area is not the same as either Lower Zambezi or offshore sediment (table 1). This is more difficult to explain, because predominantly northward littoral drift would be expected to entrain sand from the Zambezi delta, leading to homogeneous composition along the coast. Reasons for such discrepancy may include local reworking of floodplain sediments, whereas littoral drift from the north is unsupported by prevailing longshore-current

patterns (fig. 4 in Schulz et al. 2011; van der Lubbe et al. 2014).

How Does Zambezi Sand Fit with Classical Sedimentary-Petrology Theories?

The petrographic and mineralogical changes documented along the Zambezi sediment-routing system allow some considerations of consequence. In particular, they demonstrate how the knowledge acquired studying present landscapes argues against the uncritical use of simplistic concepts in geological research. In the lack of direct observations, we often try to unravel the past by using ungrounded simplifications and naive analogies (e.g., sediment that "matures" in time like fruit), unable to constrain or even imagine the complexities of past sediment-routing systems, including the effects of inheritance and multiple recycling. In the lack of clear evidence, we tend to implicitly assume that the information contained in the compositional signatures of sediments refers to the targeted sedimentary basin only, although it may—and commonly does—largely reflect tectonic or climatic conditions that existed, there or somewhere else, at earlier times. The present may well provide one key to the past, but how many are the doors and locks that this key is unable to open? Are prêt-à-porter models a help or a hindrance to the understanding of the complex four-dimensional evolution of geological entities through space and time? There are several specific questions that the present case study helps to investigate. The first one, tackled below, is: "To what extent are classical provenance models adequate?"

Provenance Models. The first model linking sand mineralogy with the tectonic setting of source areas was developed by P. Krynine (1948), who inherited from his Moscow teacher M. S. Shvetsov (1934) the belief that sediment composition reflects systematic interactions among lithogenetic processes that can be unraveled and understood. The basic assumption is that the continental crust can be envisaged as consisting of sedimentary layers nonconformably overlying deformed metamorphic rocks intruded at depth by plutonic rocks. The progressive top-down erosion of such a rocky layer cake would generate quartz-rich recycled sediments first, lithic-rich metamorphiclastic detritus next, and finally feldspar-rich plutoniclastic detritus. During a tectonically quiescent stage, recycling of cover strata would go on for a long time, eventually producing a wide sheet of quartzose sand (named "quartzite"). Conversely, tectonic uplift would lead to rapid unroofing of deep-seated plutonic rocks feeding fault-bounded basins with feldspar-rich sand (named "arkose"). These concepts were elaborated further by Krynine's student at Pennsylvania State College R. L. Folk (1980, p. 108–144), who pointed out the insufficient attention dedicated by his teacher's theory to sources of complexities such as geological inheritance, volcanism, and diversity of geodynamic settings. Furthermore, Folk acknowledged the major role of chemical weathering, and thus distinguished "climatic arkose," generated from basement rocks in dry climate even during stages of tectonic quiescence, from Krynine's "tectonic arkose."

The essence of such lines of reasoning passed largely unaltered from the pre-plate-tectonic to the post-plate-tectonic era. The same three stages identified in Krynine's and Folk's models are recognized in W. R. Dickinson's model (1985), where sediments produced in anorogenic (i.e., subduction-unrelated) settings are designated as continental block provenance, distinguished into three subprovenances: craton interior (the quartz-rich sand produced during tectonically quiescent stages), transitional, and basement uplift (the feldspar-rich sand shed from rapidly uplifted granitoid crustal blocks). Differently from Krynine's scheme, lithic-rich sediments were held to be diagnostic of orogenic (i.e., subduction-related) settings.

Heavy minerals were not organically considered in provenance models until later on (Nechaev and Isphording 1993; Garzanti and Andò 2007). One reason is that they are of limited use in ancient sediments wherever the tHM suite has been strongly depleted and modified by selective intrastratal dissolution of less durable species during diagenesis (Milliken 2007; Morton and Hallsworth 2007; Garzanti et al. 2018*a*). Moreover, the information carried by tHM suites may be profoundly distorted by hydrodynamic processes or fertility effects (Garzanti et al. 2009; Malusà et al. 2016). Heavy-mineral-rich sources such as mafic igneous and high-temperature or high-pressure metamorphic rocks have an overwhelming effect on the detrital tHM suite, heavy-mineral-poor sedimentary rocks or granite being conversely strongly underrepresented (fig. 1 in Garzanti and Andò 2019). Because of the fertility effect, the tHM suite may reflect a provenance radically different from the framework petrography, as in the Upper Zambezi where pure quartzose sand contains a clinopyroxene-dominated tHM suite.

Combining petrographic and heavy-mineral modes represents a necessary requirement to tackle the

complexities of geological landscapes and achieve a refined provenance characterization. Anorogenic provenance could thus be subdivided into volcanic and nonvolcanic, and the latter, in turn, into undissected (craton interior), transitional, and dissected (basement uplift) continental block subprovenances (Garzanti et al. 2001). Anorogenic volcanic provenance is typified by feldspatho-lithic to quartzo-feldspatho-lithic sand with rich clinopyroxene-dominated tHM suite, undissected continental block subprovenance by quartzose sand with poor ZTR-dominated tHM suite, and dissected continental block subprovenance by quartzo-feldspathic sand with rich hornblende-dominated tHM suite (Garzanti 2016). Supply from continental flood basalts such as the Karoo (anorogenic volcanic provenance) is not contemplated in Dickinson's (1985) model. Consequently, in a hypothetical analogous ancient case study, the uncritical use of that model would erroneously ascribe the compositional trend observed downstream the Upper Zambezi to mixing with arc-derived detritus.

Are models right or wrong? Obviously neither. As any tool, they apply well to some circumstances and badly to others. Because they are derived from one setting and extrapolated to another, and because different settings are not the same by definition, models are bound to be partly misleading even in the luckiest case (Garzanti and Sternai 2020). Their uncritical use is therefore discouraged.

The Final Signature of Zambezi Sand. The Zambezi River carries to the Indian Ocean quartzo-feldspathic sand, a fingerprint that has hardly an equivalent among the world's big rivers (Potter 1978; Garzanti 2019). Such a composition compares with that of granitoid-derived sand generated in dry southern California (table 3 in Dickinson 1985) and represents a typical mark of dissected continental block subprovenance. Shire sand is the richest in feldspars and thus a good example of "ideal arkose" (Dickinson 1985).

Vast river catchments typically embrace a very wide range of rocks produced in different geodynamic settings at different times. Their sediments are thus mixtures of different provenances including a considerable fraction of recycled grains. Lower Zambezi sand—characterized by feldspar ≈ quartz, very few aphanite lithics, and a rich hornblende-dominated tHM suite largely shed first-cycle from plutonic and high-grade metamorphic rocks—represents an anomaly in this respect. One main reason, discussed further below, is that quartz-dominated sand recycled in the upper reaches is not transferred to the lower course. Detritus reaching the Indian Ocean is thus generated mostly in eastern Zimbabwe, central Mozambique, and southern Malawi, where the roots of Archean cratons and Proterozoic orogens have been uplifted and progressively eroded during the southward propagation of the East African rift (Fernandes et al. 2015). Consequently, sand composition is the same as detritus shed from midcrustal basement rocks exposed along actively uplifted and deeply dissected rift shoulders, such as those flanking the Red Sea (Garzanti et al. 2001, 2013*b*), rather than that expected for a mature passive margin.

Do Minerals "Mature" during Fluvial Transport? A widely held belief in sedimentary petrology—persistent although long demonstrated untrue (e.g., Russell 1937; Shukri 1950)—is that chemically and mechanically durable minerals must increase at the expense of unstable and less resistant minerals during long-distance fluvial transport.

Uppermost Zambezi sand consists almost entirely of quartz associated with the most durable heavy minerals zircon, tourmaline, and rutile, thus representing a good example of "highly mature" sediment (Folk 1951; Hubert 1962). In the Upper Zambezi downstream, however, mafic volcanic rock fragments increase and clinopyroxene becomes first a significant, then the main, and finally the nearly exclusive transparent heavy mineral. The progressive downstream increase of detritus derived from Karoo lavas, locally including unstable olivine, results in decreasing degree of "maturation" downstream. Decreasing "maturity" with transport distance—which sounds paradoxical because maturation is by definition intended to progress irreversibly with the passing of time—is not unusual in modern rivers wherever less durable detrital components are added downstream, as observed for instance along the Kagera River in equatorial Africa (Garzanti et al. 2013*a*).

In the Middle Zambezi, sand is notably enriched in feldspars and diverse types of rock fragments supplied by the Kafue and other tributaries draining both Precambrian orogenic belts and Permo-Triassic rift-basin fills. Composition thus becomes even less "mature." In the Lower Zambezi, owing to prominent supply from local tributaries draining midcrustal Precambrian basements, quartz content decreases further, becoming equally or even less abundant than feldspar.

The Zambezi is thus an exemplary case of a sediment-routing system along which the ratio between stable and unstable minerals (too often inappropriately portrayed as degree of "maturity"; Garzanti 2017) decreases steadily with distance. Although enhanced by the artificial segmentation

of the river course after the closure of the Kariba and Cahora Bassa dams, preventing the continuity of sand transport across the reservoirs, such a trend toward less durable mineralogical assemblages downstream is primarily a natural phenomenon reflecting the multistep evolution of the river and location of erosional foci (fig. 9).

The Zambezi progressively connected stepwise the broad low-relief southern Africa plateau underlain by thick cratonic crust and sustained by

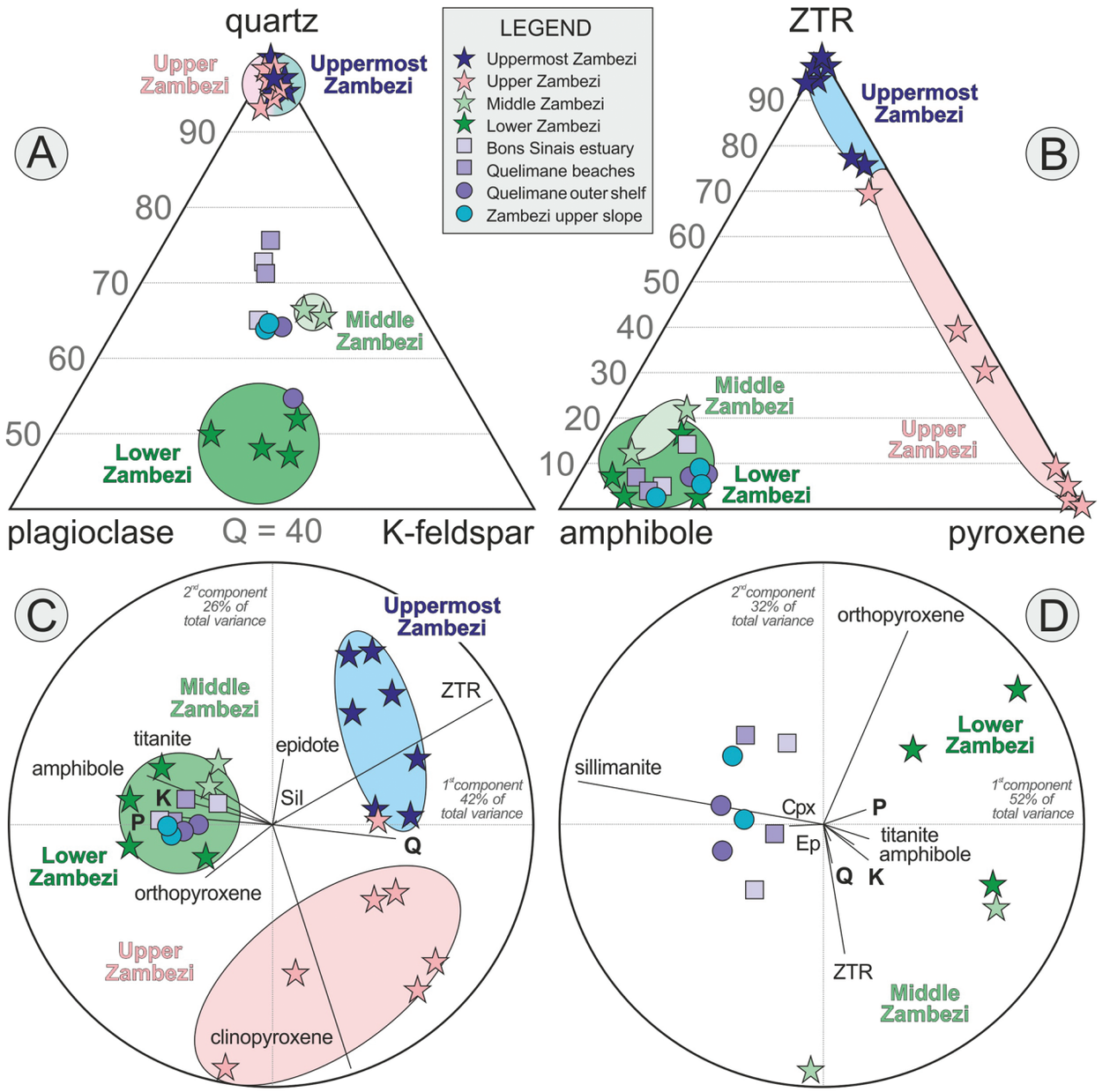

Figure 9. Zambezi River sands compared with coastal and offshore sediments. *A–C*, Uppermost and Upper Zambezi detritus is clearly distinct from any downstream sample. Sediment fed into the Indian Ocean was thus mostly derived from the middle–lower catchment even before closure of the Kariba and Cahora Bassa dams. *D*, Passive-margin sediments, however, do not closely match either Middle or Lower Zambezi sand, suggesting significant additional contribution from both the upper catchment and Mozambican lowlands in pre-Anthropocene times. Biplots *C* and *D* (Gabriel 1971) were drawn with CoDaPack software by Comas-Cufí and Thió-Henestrosa (2011). Q = quartz; P = plagioclase; K = K-feldspar; ZTR = zircon + tourmaline + rutile; Cpx = clinopyroxene; Ep = epidote; Sil = sillimanite.

dynamic uplift since mid-Cenozoic times (Lithgow-Bertelloni and Silver 1998; Moore et al. 2009*a*; Flügel et al. 2018) with the middle and lower reaches, entrenched in Karoo rifts and cutting across Precambrian mobile belts rejuvenated by the southward propagation of the East African rift in the late Neogene (Roberts et al. 2012; Hopper et al. 2020). If we just looked at the compositional signature of Lower Zambezi sand and uncritically applied traditional ideas of "maturity," disregarding the character and history of the catchment, then we would falsely infer a scenario similar to Red Sea shoulders, involving short fluvial transport from locally uplifted rift highlands. The largest river sourced in the heart of cratonic southern Africa would be left unseen.

Broken Transmission of Provenance Signals: The Anthropogenic Effect. One main reason why traditional petrological models apply so badly to the Zambezi is the pronounced segmentation of the fluvial system, which reflects its multistep Neogene evolution finally fixed by man's construction of Kariba and Cahora Bassa dams. Development of the Zambezi River is held to have started by headward erosion operated by a coastal river that captured first the Luangwa River and next the Kafue River after reincision of the Cahora Bassa and Gwembe troughs upstream. Only sometime around the early Pleistocene was the gentle-gradient Upper Zambezi captured as well, finally linking the Kalahari Plateau with the Indian Ocean via Victoria Falls (Moore et al. 2007).

Rim basins such as the Mega-Kalahari represent huge reservoirs of quartz-rich polycyclic sand stored in continental interiors. Such reservoirs may be tapped by headward-eroding coastal rivers that progressively enhance their discharge as larger segments of endorheic drainage are captured, a process continuing today with incipient piracy of the Okavango (Moore and Larkin 2001).

The undissected continental block (craton interior) subprovenance signal carried by the Upper Zambezi, however, fails to be transmitted beyond Lake Kariba. In the same way, the transitional continental block subprovenance signal carried by the Middle Zambezi fails to be transmitted downstream of Lake Cahora Bassa. The Lower Zambezi thus carries a pure dissected continental block (basement uplift) subprovenance signal to the Indian Ocean, the same that the coastal proto-Zambezi would have had before starting its inland expansion, punctuated by the progressive capture of interior drainage.

River segmentation was far less pronounced before man's intervention, as indicated by the poor compositional match between the present Lower Zambezi sand and upper Quaternary offshore sediments, which have notably higher Q/F ratio and a little more clinopyroxene. Such differences cannot be dismissed as a grain-size effect because the Q/F ratio typically increases with increasing grain size (e.g., Garzanti et al. 2021*a*) and our river samples are very fine to fine sands, whereas offshore samples are sandy silts. Rather than additional contribution by longshore-drifting sediment from outside the Zambezi delta, the plausible explanation is that a larger amount of detritus generated in the upper and middle catchment reached the ocean before closure of Kariba and Cahora Bassa dams. Forward-mixing calculations allow us to estimate that, before the Anthropocene, as much as 40% of detritus transferred to the coast was generated by erosion of Phanerozoic covers (~35% recycled from pure quartzose sand or sandstone and ~5% from basalt). Quartz-rich sand and sandstones and Karoo lavas are widespread in the Zambezi catchment, from Ngonye Falls in the Uppermost Zambezi to the lowermost course. The pre-Anthropocene contributions from the Upper or Middle Zambezi are therefore hard to accurately quantify, although the sharp mineralogical contrast between Upper Zambezi and offshore sediments indicates that most detritus was derived from the middle–lower reaches even in pre-Anthropocene times (figs. 9*A*–9*C*).

Weathering Effects Inherited from the Past. The last question dealt with here concerns the possibility to infer climate from mineralogical composition of sand. Spurred by optimism, researchers have widely used chemical indices (e.g., CIA = $[Al_2O_3/(Al_2O_3 + K_2O + Na_2O + CaO^*)] \times 100$; Nesbitt and Young 1982) or even mineralogical indices (e.g., MIA = $[Q/(Q + F)] \times 100$; Rieu et al. 2007) to infer climatic conditions in strata as old as the Paleoproterozoic. Studies of modern sedimentary systems, however, recommend caution (Garzanti and Resentini 2016). If we interpret compositional data uncritically using simplistic concepts, then we are bound to make severe mistakes.

Because feldspars are scarce in the Uppermost Zambezi ($Q/(Q + F) \geq 95\%$) and abundant in the Lower Zambezi ($Q/(Q + F) \approx 50\%$), an inconsiderate use of the MIA would suggest very humid climate in the Kalahari and very dry climate in Mozambique. Which is patently wrong. Besides being subject to marked grain-size control (Garzanti et al. 2021*a* and references therein), the $Q/(Q + F)$ ratio reaches 100% in sand of both hyperhumid equatorial Congo and hyperarid tropical Arabian or Sahara sand seas (Garzanti et al. 2013*b*, 2019*c*; Pastore et al. 2021), making it evident that climatic conditions

cannot be naively inferred by mineralogical parameters such as the MIA.

The Uppermost Zambezi and its Kwando tributary carry pure quartzose sand mostly recycled from eolian dunes that grew across the Mega-Kalahari Desert during arid stages of the Quaternary (Thomas and Shaw 2002). In a desert climate, generation of pure quartzose sand cannot occur in a single sedimentary cycle but requires widespread recycling of older sandstones affected by extensive chemical weathering in very different climatic conditions. Pure quartzose composition of sand, as well as abundant kaolinite in mud (Garzanti et al. 2014*a*), thus represents the echo of a time when sediments were produced in a chemically aggressive hot-humid climate.

In heavy-mineral suites of Uppermost Zambezi and Kwando sands, this is reflected by the scarcity of garnet relative to staurolite, kyanite, andalusite, and sillimanite (Grt/(Grt + SKA) < 5%). These minerals characterize amphibolite-facies metasedimentary rocks and unweathered detritus derived from them, where garnet is almost invariably dominant Grt/(Grt + SKA) = 70% ± 20%; Garzanti et al. 2006, 2010). This is the case for sand of the Lower Zambezi and its major tributaries (fig. 7, middle panel). In the Upper Zambezi, instead, staurolite and kyanite are common but garnet very scarce, which cannot be explained by either provenance or hydraulic factors (garnet being only slightly denser) and is most plausibly ascribed to the low stability of garnet in a humid subequatorial climate (Garzanti et al. 2013*a*). Dominance of quartz, abundance of kaolinite, and scarcity of garnet in Upper Zambezi sediment as well as in Kalahari dunes (Garzanti et al. 2014*a*, 2014*b*) thus consistently reflect humid subequatorial conditions that reigned in the past, dating back to the Cenozoic or Mesozoic, well before the arid Quaternary when Kalahari dunes invaded the landscape (Guillocheau et al. 2015, 2018).

Today, the climate is arid enough to induce only limited weathering in most of southern Africa, where detrital modes largely reflect the dominant parent lithologies exposed in source areas. In Mozambique, where the climate ranges from hot semiarid in the interior to tropical savanna downstream the Zambezi Valley (BSh to Aw classes of the Köppen climate classification), feldspars are more abundant than in any other big river on Earth. Olivine, which is considered to be a most unstable detrital mineral, occurs in small amounts both in the main stem upstream of Lake Kariba and in western tributaries joining the Zambezi shortly downstream of Cahora Bassa. Sand mineralogy thus fails to reflect a notable effect of weathering occurring at present across most of the Zambezi catchment.

Conclusions

Sand in the Uppermost Zambezi is pure quartzose and almost entirely recycled from desert dunes across the Kalahari Plateau, thus matching the theoretical sediment composition produced in cratonic interiors (undissected continental block subprovenance). At the opposite end of both the drainage basin and the petrologic spectrum of sediment shed from continental blocks, sand of the Lower Zambezi and many of its major tributaries is quartzo-feldspathic, even reaching an "ideal arkose" composition (dissected continental block subprovenance). Sand of the Middle Zambezi and its major tributaries has an intermediate feldspatho-quartzose composition (transitional continental block subprovenance). The relative abundance of durable quartz and ZTR minerals thus decreases steadily along the sediment-routing system, a trend that denies the naive but still popular idea that sediment "matures" with transport distance.

Although enhanced by the artificial segmentation of the river course after the closure of the Kariba and Cahora Bassa dams that prevented the continuity of sand transport across the reservoirs, such a downstream trend toward less durable mineralogical assemblages is primarily a natural phenomenon reflecting the dynamic uplift of the low-relief plateau of cratonic central southern Africa in the upper reaches and polyphase, ongoing rift-related rejuvenation of Precambrian mobile belts in the middle and lower reaches.

The thorough investigation of each part of the river catchment and the precise definition of the mineralogical correspondence between parent rocks and daughter sediments is indispensable to forge a key able to unlock the sedimentary archives represented by the thick stratigraphic successions accumulated throughout the late Mesozoic and Cenozoic in onshore and offshore basins and thus reconstruct with improved robustness the complex history of the Zambezi River.

ACKNOWLEDGMENTS

The article benefited from careful reviews by M. Hinderer and E. Le Pera. We are very grateful to S. K. Rasmeni and B. Zhao for their fundamental contribution to the sampling campaign, and to captains, crew, and scientists of the PAMELA-MOZ04

survey onboard the RV *Pourquoi pas?* which allowed us to collect the offshore samples. The oceanographic PAMELA-MOZ04 cruise was part of the PAMELA (Passive Margin Exploration Laboratories) scientific project led by IFREMER and TOTAL in collaboration with the Université de Bretagne Occidentale, Université Rennes 1, Université Pierre and Marie Curie, Centre national de la recherche scientifique (CNRS), and Institut Français du Pétrole et des Energies Nouvelles (IFPEN). Estuary and beach samples from the Quelimane area were kindly provided by C. de Carvalho Matsinhe (Tongji Univeristy, Shanghai). Funding was contributed by the National Research Foundation of South Africa (NRF), Water Research Commission of South Africa (WRC), African Institute of Mathematical Sciences (AIMS), and Project Ministero dell'Istruzione, dell'Università e della Ricerca (MIUR)—Dipartimenti di Eccellenza 2018–2022, Department of Earth and Environmental Sciences, University of Milano-Bicocca.

SUPPLEMENTARY MATERIAL

Supplementary data associated with this article include information on sampling sites (table A1), together with the complete bulk-sand petrography (table A2) and heavy-mineral data sets (table A3). The Google Earth map of sampling sites Zambezi .kmz is also provided.

DATA AVAILABILITY

Sediment cores collected offshore of Mozambique are curated at the IFREMER core repository in Plouzané, France. Core data related to this article can be requested at http://igsn.org/BFBGX-85862 (core MOZ4-CS14: IGSN BFBGX-85862) and http://igsn.org/BFBGX-85865 (core MOZ4-CS17: IGSN BFBGX-85865).

REFERENCE CITED ONLY IN THE APPENDIX

Garzanti, E., and Vezzoli, G. 2003. A classification of metamorphic grains in sands based on their composition and grade. J. Sediment. Res. 73:830–837.

REFERENCES CITED

Andò, S.; Morton, A.; and Garzanti, E. 2014. Metamorphic grade of source rocks revealed by chemical fingerprints of detrital amphibole and garnet. *In* Scott, R. A.; Smyth, H. R.; Morton, A. C.; and Richardson, N., eds. Sediment provenance studies in hydrocarbon exploration and production. Geol. Soc. Lond. Spec. Publ. 386:351–371.

Banks, N. L.; Bardwell, K. A.; and Musiwa, S. 1995. Karoo Rift basins of the Luangwa Valley, Zambia. *In* Lambiase, J. J., ed. Hydrocarbon habitat in rift basins. Geol. Soc. Lond. Spec. Publ. 80:285–295.

Beiersdorf, H.; Kudrass, H. R.; and von Stackelberg, U. 1980. Placer deposits of ilmenite and zircon on the Zambezi Shelf. Geol. Jahrb. D36:5–85.

Bicca, M. M.; Philipp, R. P.; Jelinek, A. R.; Ketzer, J. M. M.; dos Santos Scherer, C. M.; Jamal, D. L.; and dos Reis, A. D. 2017. Permian–Early Triassic tectonics and stratigraphy of the Karoo Supergroup in northwestern Mozambique. J. Afr. Earth Sci. 130:8–27.

Boniface, N., and Appel, P. 2018. Neoproterozoic reworking of the Ubendian Belt crust: implication for an orogenic cycle between the Tanzania Craton and Bangweulu Block during the assembly of Gondwana. Precambrian Res. 305:358–385.

Catuneanu, O.; Wopfner, H.; Eriksson, P. G.; Cairncross, B.; Rubidge, B. S.; Smith, R. M. H.; and Hancox, P. J. 2005. The Karoo basins of south-central Africa. J. Afr. Earth Sci. 43(1–3):211–253.

Collins, A. S.; Reddy, S. M.; Buchan, C.; and Mruma, A. 2004. Temporal constraints on Palaeoproterozoic eclogite formation and exhumation (Usagaran Orogen, Tanzania). Earth Planet. Sci. Lett. 224(1–2):175–192.

Comas-Cufí, M., and Thió-Henestrosa, F. S. 2011. CoDaPack 2.0: a stand-alone, multi-platform compositional software. http://ima.udg.edu/codapack/.

Cox, K. G. 1989. The role of mantle plumes in the development of continental drainage patterns. Nature 342:873–877.

Debruyne, D.; Hulsbosch, N.; Van Wilderode, J.; Balcaen, L.; Vanhaecke, F.; and Muchez, P. 2015. Regional geodynamic context for the Mesoproterozoic Kibara Belt (KIB) and the Karagwe-Ankole Belt: evidence from geochemistry and isotopes in the KIB. Precambrian Res. 264:82–97.

Derricourt, R. M. 1976. Regression rate of the Victoria Falls and the Batoka Gorge. Nature 264:23–25.

De Waele, B.; Fitzsimons, I. C. W.; Wingate, M. T. D.; Tembo, F.; Mapani, B.; and Belousova, E. A. 2009. The geochronological framework of the Irumide Belt: a prolonged crustal history along the margin of the Bangweulu Craton. Am. J. Sci. 309(2):132–187.

De Waele, B.; Kampunzu, A. B.; Mapani, B. S. E.; and Tembo, F. 2006. The Mesoproterozoic Irumide Belt of Zambia. J. Afr. Earth Sci. 46(1–2):36–70.

Dickinson, W. R. 1985. Interpreting provenance relations from detrital modes of sandstones. *In* Zuffa, G. G., ed. Provenance of arenites. Dordrecht, Reidel, NATO ASI Series 148:333–361.

Doyle, L. J.; Cleary, W. J.; and Pilkey, O. H. 1968. Mica: its use in determining shelf-depositional regimes. Mar. Geol. 6:381–389.

Droz, L., and Mougenot, D. 1987. Mozambique upper fan: origin of depositional units. Am. Assoc. Pet. Geol. Bull. 71(11):1355–1365.

Ebinger, C. E., and Scholz, C. A. 2012. Continental rift basins: the East African perspective. *In* Busby, C., and Azor, A., eds. Tectonics of sedimentary basins: recent advances. Oxford, Wiley-Blackwell, p. 185–208.

Eglinger, A.; Vanderhaeghe, O.; André-Mayer, A. S.; Goncalves, P.; Zeh, A.; Durand, C.; and Deloule, E. 2016. Tectono-metamorphic evolution of the internal zone of the Pan-African Lufilian orogenic belt (Zambia): implications for crustal reworking and syn-orogenic uranium mineralizations. Lithos 240:67–188.

Fernandes, P.; Cogné, N.; Chew, D. M.; Rodrigues, B.; Jorge, R. C. G. S.; Marques, J.; Jamal, D.; and Vasconcelos, L. 2015. The thermal history of the Karoo Moatize-Minjova Basin, Tete Province, Mozambique: an integrated vitrinite reflectance and apatite fission track thermochronology study. J. Afr. Earth Sci. 112:55–72.

Fierens, R.; Droz, L.; Toucanne, S.; Raisson, F.; Jouet, G.; and Babonneau, N. 2019. Late Quaternary geomorphology and sedimentary processes in the Zambezi turbidite system (Mozambique Channel). Geomorphology 334:1–28.

Fierens, R.; Toucanne, T.; Droz, L.; Jouet, G.; Raisson, F.; Jorissen, E. L.; Bayon, G.; Giraudeau, J.; and Jorry, S. J. 2020. Quaternary sediment dispersal in the Zambezi turbidite system (SW Indian Ocean). Mar. Geol. 428:106276. https://doi.org/10.1016/j.margeo.2020.106276.

Flint, J. J. 1974. Stream gradient as a function of order, magnitude, and discharge. Water Resour. Res. 10:969–973.

Flügel, T. J.; Eckardt, F. D.; and Cotterill, W. P. D. 2018. The geomorphology and river longitudinal profiles of the Congo-Kalahari Watershed. *In* Runge, J., ed. The African Neogene—climate, environments and people (Palaeoecol. Afr. 34). Leiden, CRC, p. 31–52.

Folk, R. L. 1951. Stages of textural maturity in sedimentary rocks. J. Sediment. Petrol. 21:127–130.

———. 1980. Petrology of sedimentary rocks. Austin, TX, Hemphill, 184 p.

Frimmel, H. E.; Basei, M. S.; and Gaucher, C. 2011. Neoproterozoic geodynamic evolution of SW-Gondwana: a southern African perspective. Int. J. Earth Sci. 100:323–354.

Fritz, H.; Abdelsalam, M.; Ali, K. A.; Bingen, B.; Collins, A. S.; Fowler, A. R.; Ghebreab, W.; et al. 2013. Orogen styles in the East African Orogen: a review of the Neoproterozoic to Cambrian tectonic evolution. J. Afr. Earth Sci. 86:65–106.

Gabriel, K. R. 1971. The biplot graphic display of matrices with application to principal component analysis. Biometrika 58:453–467.

Garzanti, E. 2016. From static to dynamic provenance analysis—sedimentary petrology upgraded. Sediment. Geol. 336:3–13.

———. 2017. The maturity myth in sedimentology and provenance analysis. J. Sediment. Res. 87:353–365.

———. 2019. Petrographic classification of sand and sandstone. Earth-Sci. Rev. 192:545–563.

Garzanti, E., and Andò, S. 2007. Plate tectonics and heavy-mineral suites of modern sands. *In* Mange, M. A., and Wright, D. T., eds. Heavy minerals in use (Dev. Sedimentol. 58). Amsterdam, Elsevier, p. 741–763.

———. 2019. Heavy minerals for Junior Woodchucks. Minerals 9(3):148. https://doi.org/10.3390/min9030148.

Garzanti, E.; Andò, S.; France-Lanord, C.; Limonta, M.; Borromeo, L.; and Vezzoli, G. 2019*a*. Provenance of Bengal shelf sediments: 2. Petrology and geochemistry of sand. Minerals 9:642. https://doi.org/10.3390/min9100642.

Garzanti, E.; Andò, S.; Limonta, M.; Fielding, L.; and Najman, Y. 2018*a*. Diagenetic control on mineralogical suites in sand, silt, and mud (Cenozoic Nile Delta): implications for provenance reconstructions. Earth Sci. Rev. 185:122–139.

Garzanti, E.; Andò, S.; and Vezzoli, G. 2006. The continental crust as a source of sand (Southern Alps cross-section, northern Italy). J. Geol. 114:533–554.

———. 2009. Grain-size dependence of sediment composition and environmental bias in provenance studies. Earth Planet. Sci. Lett. 277:422–432.

Garzanti, E.; Bayon, G.; Dennielou, B.; Barbarano, M.; Limonta, M.; and Vezzoli, G. 2021*a*. The Congo deep-sea fan: mineralogical, REE, and Nd-isotope variability in quartzose passive-margin sand. J. Sediment. Res. 91(5):433–450. https://doi.org/10.2110/jsr.2020.100.

Garzanti, E.; Bayon, G.; Dinis, P.; Vermeesch, P.; Pastore, G.; Resentini, A.; Barbarano, M.; Ncube, L.; and Van Niekerk, H. J. Forthcoming. The segmented Zambezi sedimentary system from source to sink. 2. Geochemistry, clay minerals, and detrital zircon geochronology. J. Geol.

Garzanti, E.; Dinis, P.; Vermeesch, P.; Andò, S.; Hahn, A.; Huvi, J.; Limonta, M.; et al. 2018*b*. Dynamic uplift, recycling, and climate control on the petrology of passive-margin sand (Angola). Sediment. Geol. 375:86–104.

Garzanti, E.; Dinis, P.; Vezzoli, G.; and Borromeo, L. 2021*b*. Sand and mud generation from Paraná-Etendeka continental flood basalts in contrasting climatic conditions (Uruguay vs. Namibia). Sedimentology. https://doi.org/10.1111/sed.12902.

Garzanti, E.; He, J.; Barbarano, M.; Resentini, A.; Li, C.; Yang, L.; Yang, S.; and Wang, H. 2021*c*. Provenance versus weathering control on sediment composition in tropical monsoonal climate (South China)—2. Sand petrology and heavy minerals. Chem. Geol. 564:119997. https://doi.org/10.1016/j.chemgeo.2020.119997.

Garzanti, E.; Limonta, M.; Vezzoli, G.; An, W.; Wang, J.; and Hu, X. 2019*b*. Petrology and multimineral fingerprinting of modern sand generated from a dissected magmatic arc (Lhasa River, Tibet). *In* Ingersoll, R. V.; Lawton, T. F.; and Graham, S. A., eds. Tectonics, sedimentary basins, and provenance: a celebration of William R. Dickinson's career. Geol. Soc. Am. Spec. Pap. 540:197–221. https://doi.org/10.1130/2018.2540(09).

Garzanti, E.; Padoan, M.; Andò, S.; Resentini, A.; Vezzoli, G.; and Lustrino, M. 2013*a*. Weathering and relative durability of detrital minerals in equatorial climate: sand petrology and geochemistry in the East African Rift. J. Geol. 121:547–580.

Garzanti, E.; Padoan, M.; Setti, M.; López-Galindo, A.; and Villa, I. M. 2014*a*. Provenance versus weathering control on the composition of tropical river mud (southern Africa). Chem. Geol. 366:61–74.

Garzanti, E., and Resentini, A. 2016. Provenance control on chemical indices of weathering (Taiwan river sands). Sediment. Geol. 336:81–95.

Garzanti, E.; Resentini, A.; Andò, S.; Vezzoli, G.; and Vermeesch, P. 2015. Physical controls on sand composition and relative durability of detrital minerals during long-distance littoral and eolian transport (Namibia and southern Angola). Sedimentology 62:971–996. https://doi.org/10.1111/sed.12169.

Garzanti, E.; Resentini, A.; Vezzoli, G.; Andò, S.; Malusà, M.; and Padoan, M. 2012. Forward compositional modelling of Alpine orogenic sediments. Sediment. Geol. 280:149–164.

Garzanti, E.; Resentini, A.; Vezzoli, G.; Andò, S.; Malusà, M. G.; Padoan, M.; and Paparella, P. 2010. Detrital fingerprints of fossil continental-subduction zones (axial belt provenance, European Alps). J. Geol. 118:341–362.

Garzanti, E., and Sternai, P. 2020. Against steady state: a quixotic plea for science. Earth ArXiv. https://eartharxiv.org/p9xq7/; https://doi.org/10.31223/osf.io/p9xq7.

Garzanti, E.; Vermeesch, P.; Andò, S.; Botti, E.; Limonta, M.; Vezzoli, G.; Dinis, P.; et al. 2019*c*. Congo river sand and the equatorial quartz factory. Earth-Sci. Rev. 197:102918. https://doi.org/10.1016/j.earscirev.2019.102918.

Garzanti, E.; Vermeesch, P.; Andò, S.; Vezzoli, G.; Valagussa, M.; Allen, K.; Khadi, K. A.; and Al-Juboury, I. A. 2013*b*. Provenance and recycling of Arabian desert sand. Earth Sci. Rev. 120:1–19.

Garzanti, E.; Vermeesch, P.; Padoan, M.; Resentini, A.; Vezzoli, G.; and Andò, S. 2014*b*. Provenance of passive-margin sand (southern Africa). J. Geol. 122:17–42.

Garzanti, E.; Vezzoli, G.; Andò, S.; and Castiglioni, G. 2001. Petrology of rifted-margin sand (Red Sea and Gulf of Aden, Yemen). J. Geol. 109:277–297.

Glynn, S. M.; Master, S.; Wiedenbeck, M.; Davis, D. W.; Kramers, J. D.; Belyanin, G. A.; Frei, D.; and Oberthür, T. 2017. The Proterozoic Choma-Kalomo Block, SE Zambia: exotic terrane or a reworked segment of the Zimbabwe Craton? Precambrian Res. 298:421–438.

Goscombe, B.; Foster, D. A.; Gray, D.; and Wade, B. 2020. Assembly of central Gondwana along the Zambezi Belt: metamorphic response and basement reactivation during the Kuunga Orogeny. Gondwana Res. 80:410–465.

Grantham, G. H.; Marques, J.; Wilson, M.; Manhiça, V.; and Hartzer, F. 2011. Explanation of the geological map of Mozambique, 1 : 1 000 000. Maputo, Direcção Nacional de Geologia, 383 p.

Guillocheau, F.; Chelalou, R.; Linol, B.; Dauteuil, O.; Robin, C.; Mvondo, F.; Callec, Y.; and Colin, J. P. 2015. Cenozoic landscape evolution in and around the Congo Basin: constraints from sediments and planation surfaces. *In* de Wit, M. J.; Guillocheau, F.; and de Wit, M. J. C., eds. Geology and resource potential of the Congo Basin (Reg. Geol. Rev.). Berlin, Springer, p. 271–313.

Guillocheau, F.; Simon, B.; Baby, G.; Bessin, P.; Robin, C.; and Dauteuil, O. 2018. Planation surfaces as a record of mantle dynamics: the case example of Africa. Gondwana Res. 53:82–98.

Gumbricht, T.; McCarthy, T. S.; and Merry, C. L. 2001. The topography of the Okavango Delta, Botswana, and its sedimentological and tectonic implications. S. Afr. J. Geol. 104:243–264.

Haddon, I. G., and McCarthy, T. S. 2005. The Mesozoic–Cenozoic interior sag basins of Central Africa: the Late-Cretaceous–Cenozoic Kalahari and Okavango basins. J. Afr. Earth Sci. 43:316–333.

Hanson, R. E. 2003. Proterozoic geochronology and tectonic evolution of southern Africa. *In* Yoshida, M.; Windley, B. F.; and Dasgupta, S., eds. Proterozoic East Gondwana: supercontinent assembly and breakup. Geol. Soc. Lond. Spec. Publ. 206:427–463.

Hanson, R. E.; Harmer, R. E.; Blenkinsop, T. G.; Bullen, D. S.; Dalziel, I. W. D.; Gose, W. A.; Hall, R. P.; et al. 2006. Mesoproterozoic intraplate magmatism in the Kalahari Craton: a review. J. Afr. Earth Sci. 46:141–167.

Hargrove, U. S.; Hanson, R. E.; Martin, M. W.; Blenkinsop, T. G.; Bowring, S. A.; Walker, N.; and Munyanyiwa, H. 2003. Tectonic evolution of the Zambezi orogenic belt: geochronological, structural, and petrological constraints from northern Zimbabwe. Precambrian Res. 123(2–4):159–186.

Hay, W. W. 1998. Detrital sediment fluxes from continents to oceans. Chem. Geol. 145:287–323.

Hopper, E.; Gaherty, J. B.; Shillington, D. J.; Accardo, N. J.; Nyblade, A. A.; Holtzman, B. K.; Havlin, C.; et al. 2020. Preferential localized thinning of lithospheric mantle in the melt-poor Malawi Rift. Nat. Geosci. 13(8):584–589.

Hubert, J. F. 1962. A zircon-tourmaline-rutile maturity index and the interdependence of the composition of heavy mineral assemblages with the gross composition and texture of sandstones. J. Sediment. Petrol. 32:440–450.

Ingersoll, R. V.; Bullard, T. F.; Ford, R. L.; Grimm, J. P.; Pickle, J. D.; and Sares, S. W. 1984. The effect of grain size on detrital modes: a test of the Gazzi-Dickinson point-counting method. J. Sediment. Petrol. 54:103–116.

Jacobs, J.; Pisarevsky, S.; Thomas, R. J.; and Becker, T. 2008. The Kalahari Craton during the assembly and dispersal of Rodinia. Precambrian Res. 160:142–158.

Jelsma, H. A., and Dirks, P. H. G. M. 2002. Neoarchaean tectonic evolution of the Zimbabwe Craton. *In* Fowler, C. M. R.; Ebinger, C. J.; and Hawkesworth, C. J., eds. The early Earth: physical, chemical and biological development. Geol. Soc. Lond. Spec. Publ. 199:183–211.

John, T.; Schenk, V.; Haase, K.; Scherer, E.; and Tembo, F. 2003. Evidence for a Neoproterozoic ocean in south-central Africa from mid-ocean-ridge-type geochemical signatures and pressure-temperature estimates of Zambian eclogites. Geology 31:243–246.

John, T.; Schenk, V.; Mezger, K.; and Tembo, F. 2004. Timing and PT evolution of whiteschist metamorphism in the Lufilian Arc–Zambezi Belt orogen (Zambia): implications for the assembly of Gondwana. J. Geol. 112(1):71–90.

Johnson, M. R.; Van Vuuren, C. J.; Hegenberger, W. F.; Key, R.; and Show, U. 1996. Stratigraphy of the Karoo Supergroup in southern Africa: an overview. J. Afr. Earth Sci. 23(1):3–15.

Jouet, G., and Deville, E. 2015. PAMELA-MOZ04 cruise, RV Pourquoi pas? https://doi.org/10.17600/15000700.

Jourdan, F.; Féraud, G.; Bertrand, H.; Kampunzu, A. B.; Tshoso, G.; Watkeys, M. K.; and Le Gall, B. 2005. Karoo Large Igneous Province: brevity, origin, and relation to mass extinction questioned by new $^{40}Ar/^{39}Ar$ age data. Geology 33(9):745–748.

Kampunzu, A. B.; and Cailteux, J. 1999. Tectonic evolution of the Lufilian Arc (Central Africa Copper Belt) during Neoproterozoic Pan African orogenesis. Gondwana Res. 2(3):401–421.

Key, R. M.; Cotterill, F. P. D.; and Moore, A. E. 2015. The Zambezi River: an archive of tectonic events linked to the amalgamation and disruption of Gondwana and subsequent evolution of the African Plate. S. Afr. J. Geol. 118(4):425–438.

Kinabo, B. D.; Atakwana, E. A.; Hogan, J. P.; Modisi, M. P.; Wheaton, D. D.; and Kampunzu, A. B. 2007. Early structural development of the Okavango rift zone, NW Botswana. J. Afr. Earth Sci. 48:125–136.

Klimke, J.; Franke, D.; Gaedicke, C.; Schreckenberger, B.; Schnabel, M.; Stollhofen, H.; Rose, J.; and Chaheire, M. 2016. How to identify oceanic crust—evidence for a complex break-up in the Mozambique Channel, off East Africa. Tectonophysics 693:436–452.

Knight, J., and Grab, S. W. 2018. The geomorphic evolution of southern Africa during the Cenozoic. *In* Holmes, P. J., and Boardman, J., eds. Southern African landscapes and environmental change. New York, Routledge, p. 6–28.

Kokonyangi, J. W.; Kampunzu, A. B.; Armstrong, R.; Yoshida, M.; Okudaira, T.; Arima, M.; and Ngulube, D. A. 2006. The Mesoproterozoic Kibaride belt (Katanga, SE DR Congo). J. Afr. Earth Sci. 46(1–2):1–35.

Kolla, V.; Kostecki, J. A.; Henderson, L.; and Hess, L. 1980. Morphology and Quaternary sedimentation of the Mozambique Fan and environs, southwestern Indian Oceans. Sedimentology 27:357–378.

König, M., and Jokat, W. 2010. Advanced insights into magmatism and volcanism of the Mozambique Ridge and Mozambique Basin in the view of new potential field data. Geophys. J. Int. 180(1):158–180.

Krynine, P. D. 1948. The megascopic study and field classification of sedimentary rocks. J. Geol. 56:130–165.

Leopold, L. B.; Wolman, M. G.; and Miller, J. P. 1995. Fluvial processes in sedimentology. New York, Dover, 522 p.

Le Pera, E., and Morrone, C. 2020. The use of mineral interfaces in sand-sized volcanic rock fragments to infer mechanical durability. J. Palaeogeogr. 9(1):1–26.

Lithgow-Bertelloni, C., and Silver, P. G. 1998. Dynamic topography, plate driving forces and the African superswell. Nature 395(6699):269–272.

Macgregor, D. 2018. History of the development of Permian–Cretaceous rifts in East Africa: a series of interpreted maps through time. Thematic set: tectonics and petroleum systems of East Africa. Pet. Geosci. 24:8–20. https://doi.org/10.1144/petgeo2016-155.

Main, M. 1990. Zambezi: journey of a river. Halfway House, South Africa, Southern, 313 p.

Majaule, T.; Hanson, R. E.; Key, R. M.; Singletary, S. J.; Martin, M. W.; and Bowring, S. A. 2001. The Magondi Belt in northeast Botswana: regional relations and new geochronological data from the Sua Pan area. J. Afr. Earth Sci. 32:257–267.

Malusà, M. G.; Resentini, A.; and Garzanti, E. 2016. Hydraulic sorting and mineral fertility bias in detrital geochronology. Gondwana Res. 31:1–19.

Manninen, T.; Eerola, T.; Makitie, H.; Vuori, S.; Luttinen, A.; Sénvano, A.; and Manhiça, V. 2008. The Karoo volcanic rocks and related intrusions in southern and central Mozambique. Geol. Surv. Finl. Spec. Pap. 48:211–250.

Maselli, V.; Kroon, D.; Iacopini, D.; Wade, B. S.; Pearson, P. N.; and de Haas, H. 2019. Impact of the East African Rift System on the routing of the deep-water drainage network offshore Tanzania, western Indian Ocean. Basin Res. https://doi.org/10.1111/bre.12398.

Master, S.; Bekker, A.; and Hofmann, A. 2010. A review of the stratigraphy and geological setting of the Palaeoproterozoic Magondi Supergroup, Zimbabwe—type locality for the Lomagundi carbon isotope excursion. Precambrian Res. 182(4):254–273.

Milliken, K. L. 2007. Provenance and diagenesis of heavy minerals, Cenozoic units of the northwestern Gulf of Mexico sedimentary basin. *In* Mange, M. A., and Wright, D. T., eds. Heavy minerals in use (Dev. Sedimentol. 58). Amsterdam, Elsevier, p. 247–261.

Miramontes, E.; Jouet, G.; Thereau, E.; Bruno, M.; Penven, P.; Guerin, C.; Le Roy, P.; et al. 2020. The impact of internal waves on upper continental slopes: insights from the Mozambican margin (southwest Indian Ocean). Earth Surf. Process. Landf. 45(6):1469–1482.

Modisi, M. P.; Atekwana, E. A.; Kampunzu, A. B.; and Ngwisanyi, T. H. 2000. Rift kinematics during the incipient stages of continental extension: evidence from the nascent Okavango rift basin, northwest Botswana. Geology 28:939–942.

Moore, A. E., and Blenkinsop, T. 2002. The role of mantle plumes in the development of continental-scale drainage patterns: the southern African example revisited. S. Afr. J. Geol. 105:353–360.

Moore, A. E.; Blenkinsop, T.; and Cotterill, F. P. D. 2009*a*. Southern African topography and erosion history: plumes or plate tectonics? Terra Nova 21:310–315.

Moore, A. E.; Cotterill, F. P. D.; Broderick, T. G.; and Plowes, D. 2009*b*. Landscape evolution in Zimbabwe from the Permian to present, with implications for kimberlite prospecting. S. Afr. J. Geol. 112:65–86.

Moore, A. E.; Cotterill, F. P. D.; Main, M. P. L.; and Williams, H. B. 2007. The Zambezi River. *In* Gupta, A., ed. Large rivers: geomorphology and management. Chichester, Wiley, p. 311–332.

Moore, A. E., and Dingle, R. V. 1998. Evidence for fluvial sediment transport of Kalahari sands in central Botswana. S. Afr. J. Geol. 101:143–153.

Moore, A. E., and Larkin, P. A. 2001. Drainage evolution in south-central Africa since the breakup of Gondwana. S. Afr. J. Geol. 104:47–68.

Morrone, C.; Le Pera, E.; Marsaglia, K. M.; and De Rosa, R. 2020. Compositional and textural study of modern beach sands in the active volcanic area of the Campania region (southern Italy). Sediment. Geol. 396:105567.

Morton, A. C., and Hallsworth, C. 2007. Stability of detrital heavy minerals during burial diagenesis. *In* Mange, M. A., and Wright, D. T., eds. Heavy minerals in use (Dev. Sedimentol. 58). Amsterdam, Elsevier, p. 215–245.

Nechaev, V. P., and Isphording, W. C. 1993. Heavy mineral assemblages of continental margins as indicators of plate-tectonic environments. J. Sediment. Petrol. 63:1110–1117.

Nesbitt, H. W., and Young, G. M. 1982. Early Proterozoic climates and plate motions inferred from major element chemistry of lutites. Nature 299:715–717.

Nyambe, I. A., and Utting, J. 1997. Stratigraphy and palynostratigraphy, Karoo Supergroup (Permian and Triassic), Mid-Zambezi Valley, southern Zambia. S. Afr. J. Geol. 24:563–583.

O'Connor, P. W., and Thomas, D. S. G. 1999. The timing and environmental significance of late Quaternary linear dune development in western Zambia. Quat. Res. 52:44–55.

Partridge, T. C., and Maud, R. R. 1987. Geomorphic evolution of southern Africa since the Mesozoic. S. Afr. J. Geol. 90(2):179–208.

Pastore, G.; Baird, T.; Vermeesch, P.; Resentini, A.; and Garzanti, E. 2021. Provenance and recycling of Sahara Desert sand. Earth-Sci. Rev. 216:103606. https://doi.org/10.1016/j.earscirev.2021.103606.

Potter, P. E. 1978. Petrology and chemistry of modern big river sands. J. Geol. 86:423–449.

Resentini, A.; Goren, L.; Castelltort, S.; and Garzanti, E. 2017. Partitioning the sediment flux by provenance and tracing erosion patterns in Taiwan. J. Geophys. Res. Earth Surf. 122(7):1430–1454. https://doi.org/10.1002/2016JF004026.

Rieu, R.; Allen, P. A.; Plötze, M.; and Pettke, T. 2007. Compositional and mineralogical variations in a Neoproterozoic glacially influenced succession, Mirbat area, South Oman: implications for paleoweathering conditions. Precambrian Res. 154:248–265.

Roberts, E. M.; Stevens, N. J.; O'Connor, P. M.; Dirks, P. H. G. M.; Gottfried, M. D.; Clyde, W. C.; Armstrong, R. A.; Kemp, A. I. S.; and Hemming, S. 2012. Initiation of the western branch of the East African Rift coeval with the eastern branch. Nat. Geosci. 5(4):289–294.

Russell, R. D. 1937. Mineral composition of Mississippi River sands. Geol. Soc. Am. Bull. 48:1307–1348.

Salman, G., and Abdula, I. 1995. Development of the Mozambique and Ruvuma sedimentary basins, offshore Mozambique. Sediment. Geol. 96:7–41.

Schulz, H.; Lückge, A.; Emeis, K. C.; and Mackensen, A. 2011. Variability of Holocene to late Pleistocene Zambezi riverine sedimentation at the upper continental slope off Mozambique, 15°–21°S. Mar. Geol. 286:21–34.

Schwanghart, W., and Scherler, D. 2014. TopoToolbox 2—MATLAB-based software for topographic analysis and modeling in Earth surface sciences. Earth Surf. Dyn. 2:1–7. https://doi.org/10.5194/esurf-2-1-2014.

Shaw, A., and Goudie, A. S. 2002. Geomorphological evidence for the extension of the Mega-Kalahari into south-central Angola. S. Afr. Geogr. J. 84:182–194.

Shaw, P., and Thomas, D. S. G. 1988. Lake Caprivi: a late Quaternary link between the Zambezi and middle Kalahari drainage. Z. Geomorphol. 32:329–337.

Shukri, N. M. 1950. The mineralogy of some Nile sediments. Q. J. Geol. Soc. Lond. 105:511–534.

Shvetsov, M. S. 1934. Petrografiya osadochnykh porod [Petrography of sedimentary rocks]. Moscow-Leningrad, Gostoptekhizdat (1948), 387 p.

Söderlund, U.; Hofmann, A.; Klausen, M. B.; Olsson, J. R.; Ernst, R. E.; and Persson, P. O. 2010. Towards a complete magmatic barcode for the Zimbabwe craton: baddeleyite U-Pb dating of regional dolerite dyke swarms and sill complexes. Precambrian Res. 183(3):388–398.

Stokes, S.; Haynes, G.; Thomas, D. S. G.; Horrocks, J. L.; Higginson, M.; and Malifa, M. 1998. Punctuated

aridity in southern Africa during the last glacial cycle: the chronology of linear dune construction in the northeastern Kalahari. Palaeogeogr. Palaeoclimatol. Palaeoecol. 137:305–322.

Svensen, H.; Corfu, F.; Polteau, S.; Hammer, Ø.; and Planke, S. 2012. Rapid magma emplacement in the Karoo Large Igneous Province. Earth Planet. Sci. Lett. 325/326:1–9.

Thiéblemont, D.; Liégeois, J. P.; Fernandez-Alonso, M.; Ouabadi, A.; Le Gall, B.; Maury, R.; Jalludin, M.; et al. 2016. Geological map of Africa at 1:10M scale. Paris, CGMW-BRGM (Commission for the Geological Map of the World–Bureau de Recherches Géologiques et Minières).

Thomas, D. S. G.; O'Connor, P. W.; Bateman, M. D.; Shaw, P. A.; Stokes, S.; and Nash, D. J. 2000. Dune activity as a record of late Quaternary aridity in the northern Kalahari: new evidence from northern Namibia interpreted in the context of regional arid and humid chronologies. Palaeogeogr. Palaeoclimatol. Palaeoecol. 156:243–259.

Thomas, D. S. G., and Shaw, P. A. 1988. Late Cainozoic drainage evolution in the Zambezi basin: evidence from the Kalahari rim. J. Afr. Earth Sci. 7:611–618.

———. 1991. The Kalahari environment. Cambridge, Cambridge University Press, 284 p.

———. 2002. Late Quaternary environmental change in central southern Africa: new data, synthesis, issues and prospects. Quat. Sci. Rev. 21:783–797.

Vallier, T. L. 1974. Volcanogenic sediments and their relation to landmass volcanism and sea floor-continent movements, western Indian Ocean, Leg 25, Deep Sea Drilling Project. Initial Rep. Deep Sea Drilling Project 25:515–542.

van der Lubbe, J. J. L.; Tjallingii, R.; Prins, M. A.; Brummer, G. J. A.; Jung, S. J. A.; Kroon, D.; and Schneider, R. R. 2014. Sedimentation patterns off the Zambezi River over the last 20,000 years. Mar. Geol. 355:189–201.

von Eynatten, H.; Pawlowsky-Glahn, V.; and Egozcue, J. J. 2002. Understanding perturbation on the simplex: a simple method to better visualise and interpret compositional data in ternary diagrams. Math. Geol. 34:249–257.

Walford, H. L.; White, N. J.; and Sydow, J. C. 2005. Solid sediment load history of the Zambezi Delta. Earth Planet. Sci. Lett. 238:49–63.

Wellington, J. 1955. Southern Africa: a geographical study. Vol. 1. Physical geography, climate, vegetation and soils: hydrography. Cambridge, Cambridge University Press, 528 p.

Whipple, K. X. 2004. Bedrock rivers and the geomorphology of active orogens. Annu. Rev. Earth Planet. Sci. 32:151–185.

Zindorf, M.; Rooze, J.; Meille, C.; März, C.; Jouet, G.; Newton, R.; Brandily, C.; and Pastor, L. 2021. The evolution of early diagenetic processes at the Mozambique margin during the last glacial-interglacial transition. Geochim. Cosmochim. Acta 300:9–94.